CHAPTER 4

ANALYSIS AND DESIGN

Section I. Characteristics

4-1. Structural Behavior. The stability of a sheet pile cell results from the composite action of the soil fill and the interlocking steel piling. The structural behavior of a cellular structure is governed by the engineering properties of the cell fill and the steel pile shell that contains and stiffens the cell fill. Because of this composite action, cells cannot be classified as a traditional concrete gravity monolith or a flexible earth embankment.

4-2. Forces.

a. Applied External Forces. Steel sheet pile cells are subject to external forces resulting from static water head, wave action, lateral earth pressure, and surcharge due to live load, earthquake, etc. These forces should be computed and applied as specified in the various engineer manuals referenced in Appendix A.

b. Reactive Berm Force. The passive force developed by a berm should be determined by a wedge analysis that accounts for the intersection of the failure wedge with the back slope of the berm. The Coulomb method of analysis or a Culmann graphical solution can be used when appropriate. The resistance provided by the berm should be limited to a value consistent with the berm reaction resulting from a sliding analysis.

4-3. Equivalent Cell Width. The equivalent width B of a sheet pile cellular structure is defined as the width of an equivalent rectangular section having a section modulus equal to that of the actual structure. For design purposes this definition can be simplified to equivalent areas as follows:

$$B = \frac{A}{2L}$$

where

B = equivalent width

A = area of main cell, plus one connecting cell

2L = center-to-center distance between main cells

See Figure 4-1.

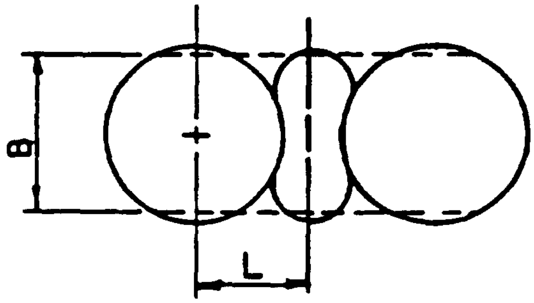

a. Plan circular cell

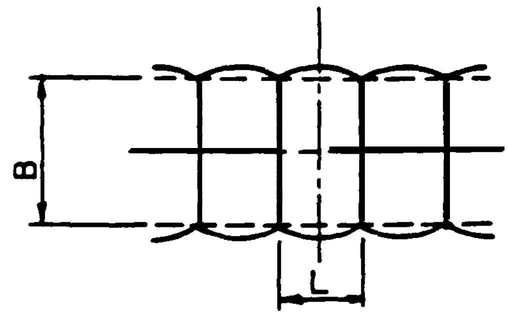

b. Plan arc and diaphragm cell

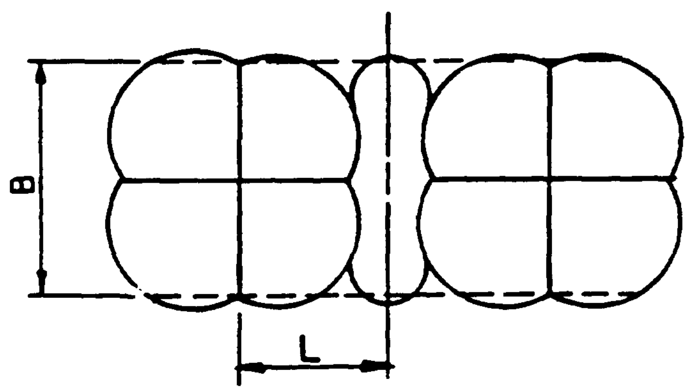

c. Plan clover leaf cell

Figure 4-1. Typical cellular cofferdam geometry

Section II. Loading Conditions

4-4. Cofferdams. The following loading conditions and requirements must be investigated:

a. Case I, Maximum Pool Condition. River pool to top of cell; cell fill saturation line assumed to slope from top outboard face of the cell to the inboard face, the slope being dependent upon the type of fill, the presence of a berm, and any positive measures taken to control the phreatic surface in the cell or the berm such as weep holes in the cell or drains and pumped wells in the berm, Figure 4-2a. It should be emphasized that the saturation level within the cell fill is perhaps the single most important consideration in the design of the cells; therefore, its location must be estimated with extreme care.

b. Case II, Initial Filling Condition. Balanced pools on both the inside and outside of the cofferdam; for determination of maximum interlock stress, cell fill is assumed to be completely saturated to top of cell unless positive measures are taken to preclude fill saturation, Figure 4-2b.

c. Case III, Drawdown Condition. Pool level inside cofferdam some specified distance below pool level outside cofferdam; cell fill saturation level varies uniformly between the outside pool level and some specified distance above the pool level inside the cofferdam, Figure 4-2c. This condition is checked to determine the maximum rate of dewatering. This condition can be critical for stability and interlock stress. The designer establishes the maximum rate of dewatering, as influenced by the cell fill saturation level, at which level the allowable interlock stress should not be exceeded and all factors of safety should be met. Since the cell fill saturation level is critical, the actual saturation level must be monitored in the field during dewatering to verify the assumed conditions. Instructions to this effect and the critical parameters should be included in the contract specifications and/or in "Special Instructions" to the resident engineer. Note that the forces acting upon a cofferdam can change with time. For example, overburden may be present on the inside of a cofferdam when it is initially dewatered; however, the overburden may subsequently be excavated, thus perhaps adversely affecting the stability of the cofferdam. In short, loading conditions not present during construction and initial dewatering must be anticipated and taken into account during design.

4-5. Retaining Structures. Cellular-type retaining walls are designed in accordance with those loading conditions and forces specified in the engineer manuals listed in Appendix A. The application of these loading criteria is basically the same if the structure is constructed of mass concrete or is a sheet pile cell filled with soil, the exception being that cells are not rigid structures; therefore, they should be designed for active earth backfill pressures. The most critical element in designing a stable cellular retaining structure is the degree of saturation of the cell fill. Consequently, the design should be based on the worst saturation condition both during construction and in-service.

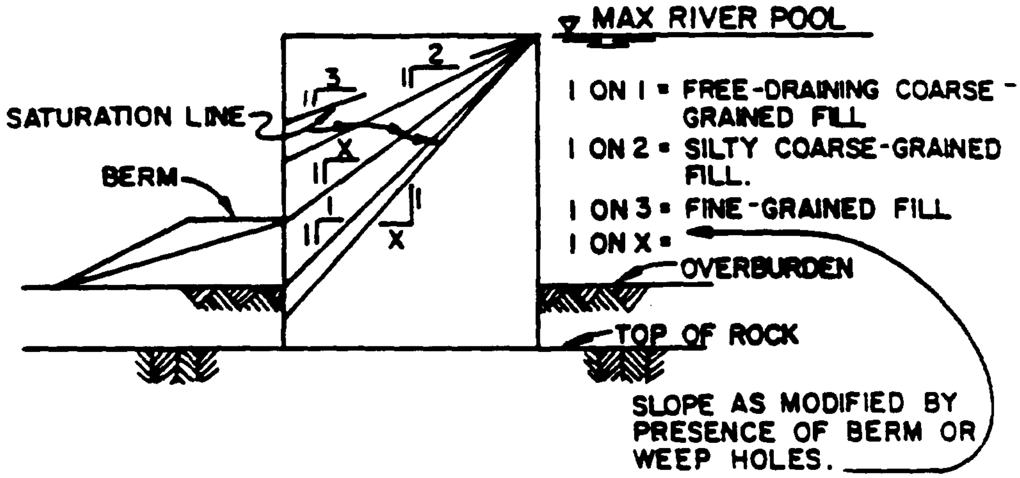

a. Case I, maximum pool condition

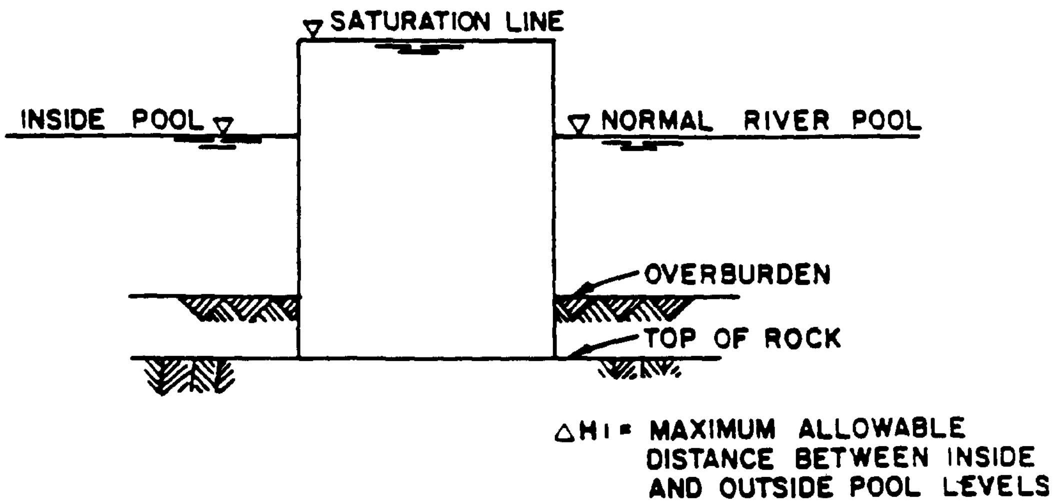

b. Case II, initial filling condition

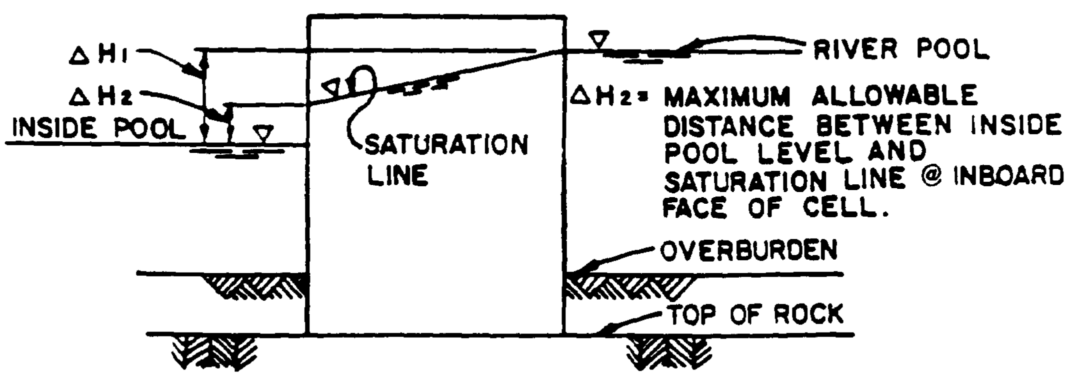

c. Case III, drawdown condition

Figure 4-2. Cofferdam loading conditions

4-6. Mooring Cells. Mooring cells are individual cells designed to resist live loads due to barge impact or line pull and the accompanying earth pressures depending on the direction of loading. The magnitudes of the impact and line pull loads are dependent on such circumstances as the size of tows, tow winch capacity, and other similar considerations. Attention should be paid to special loading cases such as fill placed hydraulically during construction, the placement of which could govern design because of the high interlock stresses due to the saturated fill.

4-7. Lock Walls. Cellular lock walls, including chamber walls and approach-type walls, are designed in accordance with the loading conditions outlined in the engineer manuals listed in Appendix A. Essentially, land lock walls are a special type of retaining wall and, due to the rapidly fluctuating pool of the lock chamber, care must be taken in establishing the most severe saturation condition for each load case. The degree of saturation of the cell fill is critical in the design. Controlling load cases must be determined for the various types of walls for which cells are adaptable. These include lock chamber land, river, and intermediate walls, and upper and lower approach walls.

4-8. Spillway Weirs. Cellular fixed weir structures consist of circular cells and connecting areas filled with rock or other granular material topped off by a concrete cap with a fixed concrete crest. Because of the flow over the weir, permanent upstream and downstream rock berms extending the full height of the cells are usually constructed for stability and scour prevention. In-service lateral loads are produced by upper and lower pool levels, earth pressures, and such special considerations as earthquake and ice thrust. Maximum interlock stresses will probably occur in the construction condition when the cells are filled and before the berms are built. Again, cell fill saturation is critical in designing for interlock stresses, especially if the cells are hydraulically filled or if construction is in the wet with the possibility of a rapidly fluctuating river.

Section III. Analysis of Failure Modes

4-9. External Cell Stability.

a. Sliding. For design and investigation of sheet pile cellular structures, the procedures outlined in the following paragraphs should be used to assess sliding stability on rock and soil foundations.

(1) Design Process. An adequate assessment of sliding stability must account for the basic structural behavior, the mechanism of transmitting compressive and shearing loads to the foundation, the reaction of the foundation to such loads, and the secondary effects of the foundation behavior on the structure. A fully coordinated team of geotechnical and structural engineers and geologists should ensure that the results of the sliding analyses are properly integrated into the design. Critical aspects of the design process which require coordination include: preliminary estimates of geotechnical data, subsurface conditions, and type of structure; selection of loading

conditions, loading effects, potential failure mechanisms, and other related features of the analytical models; evaluation of the technical and economic feasibility of alternative structures; refinement of the preliminary design to reflect the results of detailed geotechnical site explorations, laboratory testing, and numerical analyses; and modification of the structure during construction due to unexpected variations in the foundation conditions.

(2) Method of Analysis. The sliding analysis is based on the principles of structural and geotechnical mechanics, which apply a safety factor to the material strength parameters in a manner that places the forces acting on the structure and foundation wedges in sliding equilibrium. The factor of safety (FS) is defined as the ratio of the shear strength and the applied shear stress as follows.

$$FS = \frac{\tau_F}{\tau}$$

and

$$\frac{\tau_F}{FS} = \frac{\sigma \tan \phi}{FS} + \frac{c}{FS}$$

where

τ_F = shear strength

τ = applied shear stress

σ = normal stress

ϕ = angle of shearing resistance, or internal friction

c = cohesion

See Figure 4-3. A sliding mode of failure will occur along a presumed failure surface when the applied shearing force exceeds the resisting shearing forces. The failure surface can be any combination of plane and curved surfaces, but for simplicity, all failure surfaces are assumed to be planes which form the bases of wedges. The critical failure surface with the lowest safety factor is determined by an iterative process. Sliding stability of most sheet pile cellular structures can be adequately assessed by using a limit equilibrium

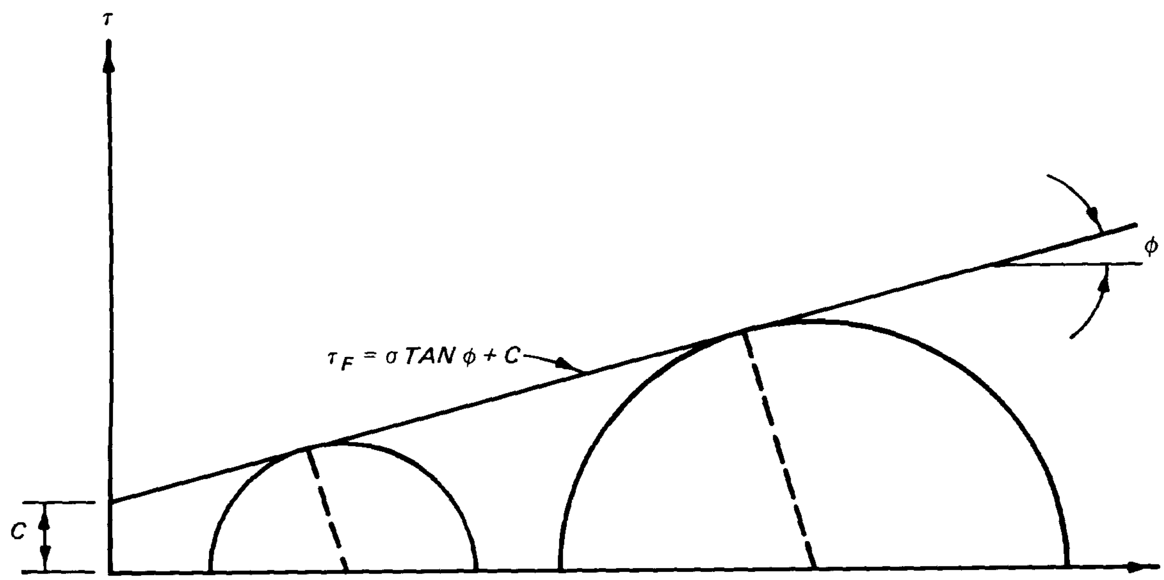

Figure 4-3. Shear strength envelope

approach. Designers must exercise sound judgment in performing these analyses. Assumptions and simplifications are as follows:

(a) A two-dimensional analysis is presented. These principles should be extended if unique, three-dimensional, geometric features and loads critically affect the sliding stability of a specific structure.

(b) Only force equilibrium is satisfied in this analysis. Moment equilibrium is not used. The shearing force acting parallel to the interface of any two wedges is assumed to be negligible. Therefore, the portion of the failure surface at the bottom of each wedge is loaded only by the forces directly above or below it. There is no interaction of vertical effects between the wedges.

(c) Analyses are based on assumed plane failure surfaces. The calculated safety factor will be realistic only if the assumed failure mechanism is kinematically possible.

(d) Considerations regarding displacements are excluded from the limit equilibrium approach. The relative rigidity of different foundation materials and the sheet pile cellular structure may influence the results of the sliding stability analysis. Such complex structure-foundation systems may require a more intensive sliding investigation than a limit equilibrium approach. The effects of strain compatibility along the assumed failure surface may be included by interpreting data from in situ tests, laboratory tests, and finite element analyses.

(e) A linear relationship is assumed between the resisting shearing force and the normal force acting along the failure surface beneath each wedge.

(3) Multiwedge System Analysis. A general procedure for analyzing multiwedge systems includes:

(a) Assuming a potential failure surface which is based on the stratification, location and orientation, frequency and distribution of discontinuities of the foundation material, and the configuration of the structure.

(b) Dividing the assumed slide mass into a number of wedges, including a single structural wedge.

(c) Drawing free body diagrams which show all the forces assumed to be acting on each wedge.

(d) Solving for the safety factor by direct or iterative methods. A derivation of the governing wedge equation for a typical wedge is shown in Appendix B. The governing wedge equation is

$$(P_{i-1} - P_i) = \frac{\left[(W_i + V_i)\cos\alpha_i - U_i + (H_{Li} - H_{Ri})\sin\alpha_i\right]\dfrac{\tan\phi_i}{FS_i}}{\cos\alpha_i - \sin\alpha_i\dfrac{\tan\phi_i}{FS_i}}$$

$$\frac{(H_{Li} - H_{Ri})\cos\alpha_i + (W_i + V_i)\sin\alpha_i + \dfrac{c_i}{FS_i} L_i}{\cos\alpha_i - \sin\alpha_i\dfrac{\tan\phi_i}{FS_i}}$$

where

i = number of wedges

$(P_{i-1} - P_i)$ = summation of applied forces acting horizontally on the i^{th} wedge. (A negative value for this term indicates that the applied forces acting on the i^{th} wedge exceed the forces resisting sliding along the base of the wedge. A positive value for the term indicates that the applied forces acting on the i^{th} wedge are less than the forces resisting sliding along the base of that wedge.)

W_i = total weight of water, soil, rock, etc., in the i^{th} wedge

V_i = any vertical force applied above top of the i^{th} wedge

α_i = angle between the inclined plane of the potential failure surface of the i^{th} wedge and the horizontal (positive is counterclockwise)

U_i = uplift force exerted along the failure surface of the i^{th} wedge

H_{Li} = any horizontal force applied above the top or below the bottom of the left-side adjacent wedge

H_{Ri} = any horizontal force applied above the top or below the bottom of the right-side adjacent wedge

ϕ_i = angle of shearing resistance or internal friction of the i^{th} wedge

c_i = cohesion or adhesion, whichever is the smaller on the potential failure surface of the i^{th} wedge. (Cohesion should not exceed the adhesion at the structure-foundation interface.)

L_i = length along the failure surface of the i^{th} wedge

The governing equation applies to the individual wedges. For a system of wedges to act as an integral failure mechanism, the factors of safety (FS) for all wedges must be identical, therefore

$$FS_1 = FS_2 = \ldots FS_{i-1} = FS_i = FS_{i+1} = \ldots FS_N$$

where N = number of wedges in the failure mechanism. The actual FS for sliding equilibrium is determined by satisfying overall horizontal equilibrium ($\Sigma F_H = 0$) for the entire system of wedges; therefore

$$\sum_{i=1}^{N} (P_{i-1} - P_i) = 0$$

and $P_o = P_N = 0$. Usually an iterative solution process is used to determine the actual FS for sliding equilibrium. The analysis proceeds by assuming trial values of the safety factor and unknown inclinations of the slip path until the governing equilibrium conditions, failure criterion, and definition of FS are satisfied. An analytical or a graphical procedure may be used for this iterative solution.

(4) Design Considerations. Some special considerations for applying the general wedge equation to specific site conditions are discussed below.

(a) The interface between the group of active wedges and the structural wedge is assumed to be a vertical plane located at the heel of and extending to the base of the structural wedge. The magnitudes of the active forces depend on the actual values of the FS and the inclination angles, a α , of the slip path. The inclination angles, corresponding to the maximum active forces for each potential failure surface, can be determined by independently analyzing the group of active wedges for a trial FS. In rock, the inclination may be predetermined by discontinuities in the foundation. The general equation only applies directly to active wedges with assumed horizontal active forces,

(b) The governing wedge equation is based on the assumption that shearing forces do not act on the vertical wedge boundaries; hence there can only be one structural wedge because the structure transmits significant shearing forces across vertical internal planes. Discontinuities in the slip path beneath the structural wedge should be modeled by assuming an average slip plane along the base of the structural wedge.

(c) The interface between the group of passive wedges and the structural wedge is assumed to be a vertical plane located at the toe of the structural wedge and extending to the base of the structural wedge. The magnitudes of the passive forces depend on the actual values of the safety factor and the inclination angles of the slip path. The inclination angles, corresponding to the minimum passive forces for each potential failure mechanism, can be determined by independently analyzing the group of passive wedges for a trial safety factor. The general equation only applies directly to passive wedges with assumed horizontal passive forces.

(d) Sliding analyses should consider the effects of cracks on the active side of the structural wedge in the foundation material due to differential settlement, shrinkage, or joints in a rock mass. The depth of cracking in cohesive foundation material can be estimated in accordance with the following:

$$d_c = \frac{2c_d}{\gamma} \tan \left(45° - \frac{\phi_d}{2}\right)$$

where

d_c = depth of crack in cohesive foundation material

$c_d = \frac{c}{FS}$

$\phi_d = \tan^{-1} \left(\frac{\tan \phi}{FS}\right)$

The value d_c in a cohesive foundation cannot exceed the embedment of the structural wedge. Cracking depth in massive strong rock foundations should be assumed to extend to the base of the structural wedge. Shearing resistance along the crack should be ignored, and full hydrostatic pressure should be assumed to act at the bottom of the crack. The hydraulic gradient across the base of the structural wedge should reflect the presence of a crack at the heel of the structural wedge.

(e) The effects of seepage forces should be included in the sliding analysis. Analyses should be based on conservative estimates of uplift pressures. For the estimation of uplift pressures on the wedges, it can be assumed that the uplift pressure acts over the entire area of the base of the wedge and if seepage from headwater to tailwater can occur across a cell, the pressure head at any point should reflect the head loss due to water flowing through the medium. The approximate pressure head at any point can be determined by the line-of-seepage method, which assumes that the head loss is directly proportional to the length of the seepage path. The seepage path for the structural wedge extends from the upper surface of the untracked material adjacent to the heel of the cell, along the embedded perimeter of the structural wedge, to the upper surface adjacent to the toe of the cell. Referring to Figure 4-4, the seepage distance is defined by points "a" and "b." The pressure head at any point is equal to the elevation head minus the produce of the hydraulic gradient times the distance along the seepage path to the point in question. Estimates of pressure heads for the active and passive wedges should be consistent with those of the heel and toe of the structural wedge. Uplift pressures can be reduced by pressure relief systems. The pressure heads acting on the wedges developed from the line-of-seepage analysis should be modified to reflect the effects of pressure relief systems. Uplift forces used for the sliding analyses should be selected in consideration of conditions which are presented in the applicable design memoranda. For a more detailed discussion of the line-of-seepage method, refer to EM 1110-2-2501. For the majority of structural stability computations, the line-of-seepage method is considered to be sufficiently accurate. However, there may be special situations where the flow net method is required to evaluate seepage forces.

(5) Seismic Sliding Stability. The sliding stability of a sheet pile cellular structure for an earthquake-induced base motion should be checked by assuming that the specified horizontal earthquake acceleration, and the vertical earthquake acceleration if in the analysis, will act in the most unfavorable direction. The earthquake-induced forces on the structure and foundation wedges can then be determined by a rigid body analysis. The horizontal earthquake acceleration can be obtained from seismic zone maps (ER 1110-2-1806) or, in the case where a design earthquake has been specified for the structure, an acceleration developed from analysis of the design earthquake. The vertical earthquake acceleration is normally neglected but can be taken as two-thirds of the horizontal acceleration, if included in the analysis. The added mass of the retained pool and soil can be approximated by Westergaard's parabola (EM 1110-2-2200), and the Mononobe-Okabe method (EM 1110-2-2502),

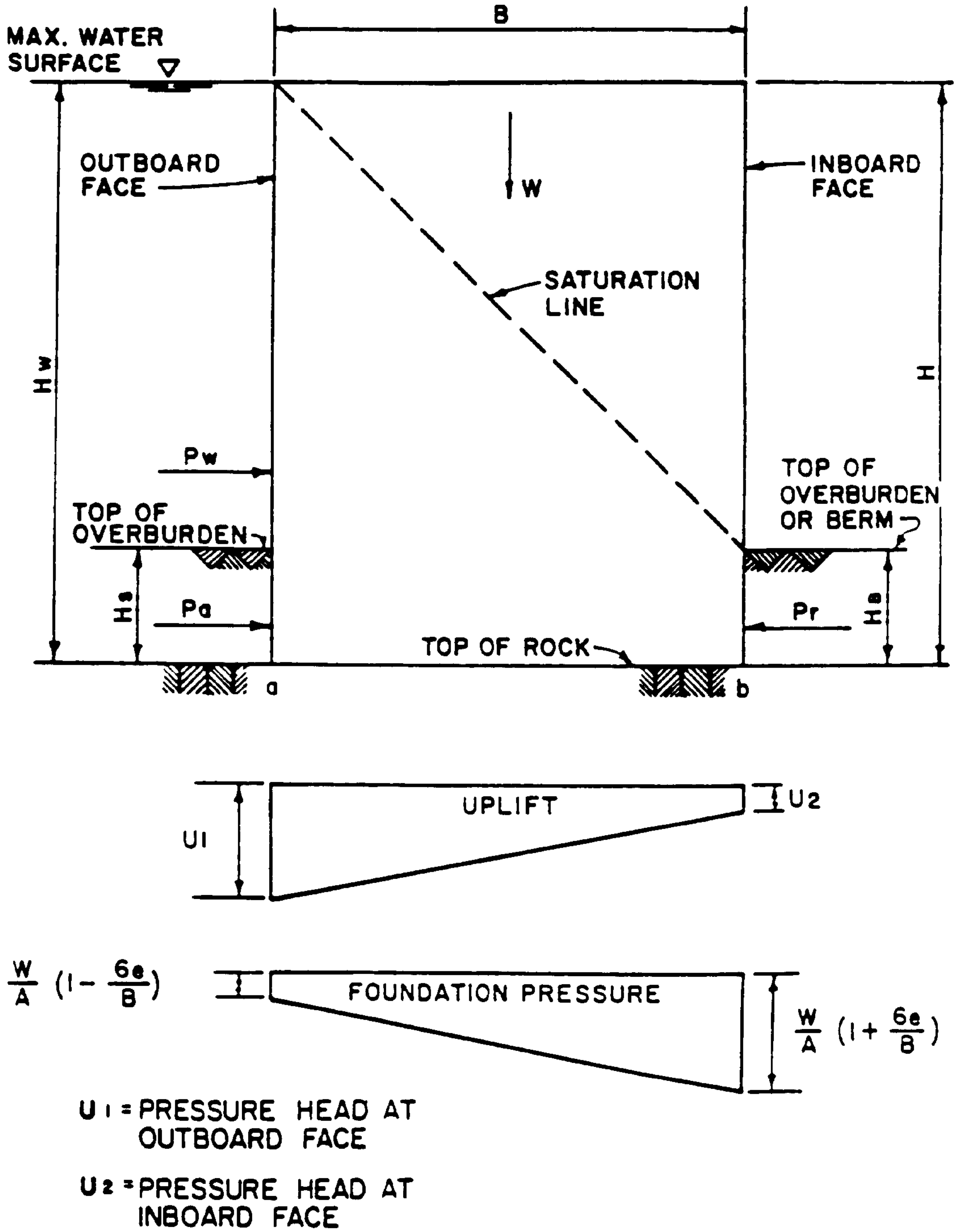

Figure 4-4. Overturning stability, typical loading and nomenclature

respectively. The structure should be designed for a simultaneous increase in force on one side and decrease on the opposite side of the cell when such can occur.

b. Overturning. A soil-filled cellular structure is not a rigid gravity structure that could fail by overturning about the toe of the inboard side. Before overturning could occur, the structure must have failed from causes such as pullout of the sheet piles at the heel and subsequent loss of cell fill. Nevertheless, a gravity-block analysis may serve as a starting point for determining the required cell diameter. Considering that the cell fill cannot resist tension, the cell should be proportioned so that the resultant of all forces falls within the middle one third of the equivalent rectangular base. This type of analysis will also serve to determine foundation pressures with

$$FP = \frac{W}{A}\left(1 \pm \frac{6e}{B}\right)$$

where

FP = computed foundation pressure

w = effective weight of cell fill

A = area of base = B x 1.0 for l-foot strip

e = eccentricity of resultant of all forces from center of cell

B = effective width of cell

See Figure 4-4. Again, it must be emphasized that overturning computations based on the gravity block concept do not give a true indication of cell stability.

c. Rotation (Hansen's Method).

(1) This method considers cellular structures to act as rigid bodies. For cells founded on rock, failure occurs along a circular sliding surface in the cell fill intercepting the toe of the sheet piles; however, for ease of calculation it is convenient to assume a logarithmic spiral of radius

$$r_\theta = r_o e^{\theta \tan \phi}$$

where

r_θ and θ = variables in the polar coordinate system

r_o = radius for $\theta = 0$

e = base of natural logarithms

ϕ = angle of internal friction of cell fill

As shown in Figure 4-5, the resultant of the unknown internal forces on the spiral will pass through the pole ω of the spiral and thus not enter into the equation of moments about the pole.

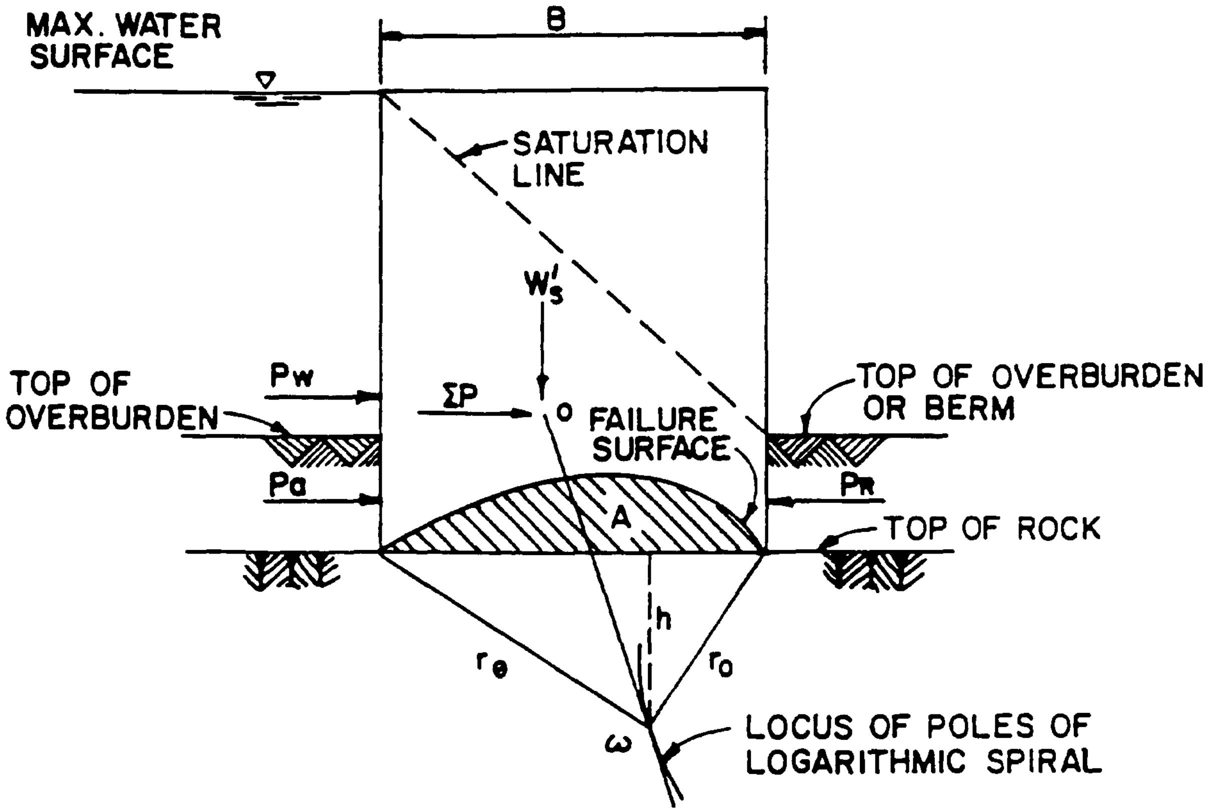

$$A = \frac{r_e^2 - r_o^2}{4 \tan \phi} - \frac{hB}{2}$$

o = INTERSECTION OF ΣP AND W'_s

oω = TANGENT FROM O TO LOCUS OF POLES OF LOGARITHMIC SPIRAL TO LOCATE ω

Figure 4-5. Rotation--Hansen's method, cell founded on rock

(2) The FS against failure is defined as the ratio of moments about the pole, that is, the ratio of the effective weight of the cell fill above the failure surface to the net overturning force. Thus

$$FS = \frac{M_B}{M_\omega}$$

where

M_B = moment about pole of W'_s

W'_s = effective weight of cell fill above failure surface

M_ω = moment about pole due to resultant overturning force ΣP

$\Sigma P = P_w + P_a - P_r$) as shown in Figure 4-5

(3) The pole of the logarithmic spiral may be found by trial until the minimum factor of safety is determined. However, since the pole of the failure spiral is on the locus of poles of the logarithmic spirals which pass through the toes of the sheet piles, the failure plane pole can be found by drawing the tangent to this locus from the intersection of W'_s and ΣP .

(4) Hansen's method, as applied to cells founded on rock, is applicable only where the rock is not influenced by discontinuities in the foundation to at least a depth h (Figure 4-5).

(5) The Hansen method of analysis for cells founded on soil is similar to that of cells founded on rock, except that the failure surface can be convex or concave, i.e., the surface of rupture can be in the cell fill or in the foundation. Both possibilities must be investigated to determine the minimum FS. The FS is defined as

$$FS = \frac{M_B}{M_\omega}$$

where

M_B = moment about pole due to ΣR

ΣR = resultant of W'_s , Pe_a , Pe_R , and U

W'_s = total weight of cell fill above failure surface

Pe_a and Pe_R = active and passive forces on embedded portion of cell, respectively

M_ω and ΣP = as previously defined

See Figure 4-6.

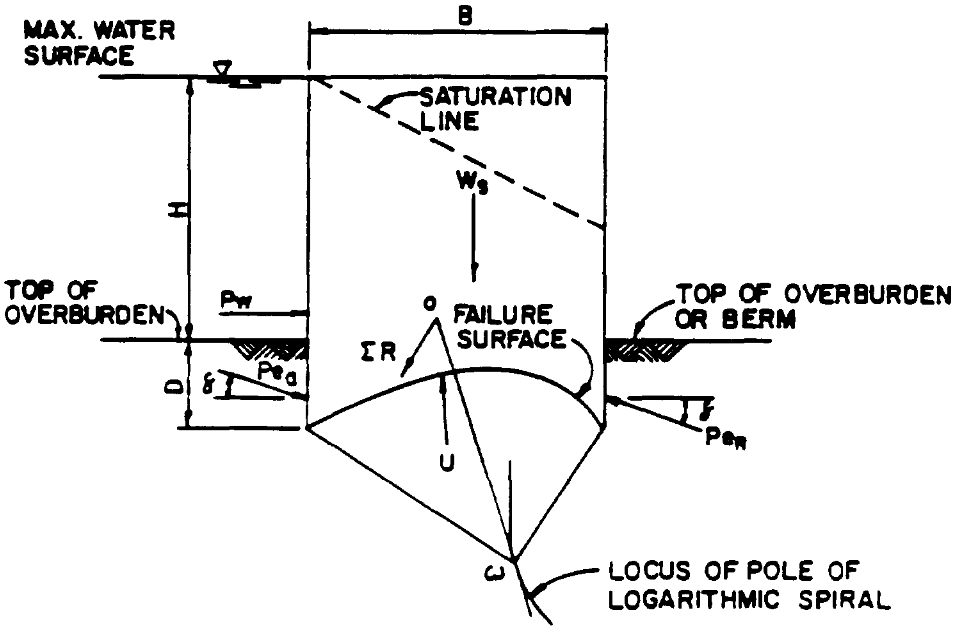

a. Rupture surface into the cell fill

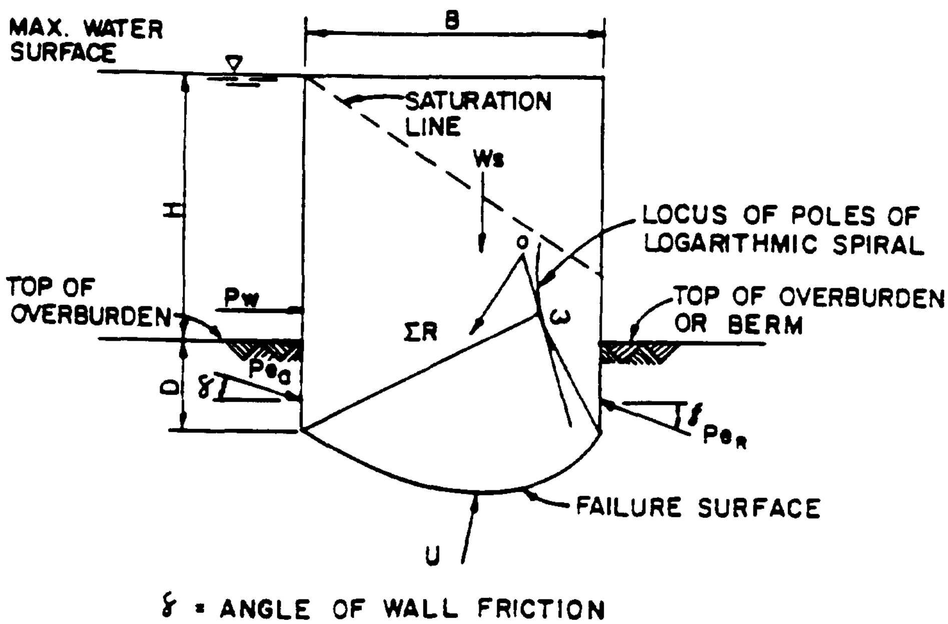

b. Rupture surface into the foundation

Figure 4-6. Rotation--Hansen's method, cell founded on soil

(6) Stability, as determined by the Hansen method, is directly related to the engineering properties of the cell fill and the foundation and properly considers the saturation level within the cell as well as seepage forces beneath the cell. This method of analysis is particularly appropriate for cells founded in overburden. A more detailed explanation of this method can be found in discussions by Hansen (item 35) and Ovesen (item 55).

4-10. Deep-Seated Sliding Analysis.

a. Introduction.

(1) Sliding stability has been discussed in Paragraph 4.9a. In general, a cell on rock will very rarely fail on its base, probably because of friction of the fill and anchoring of the sheet pile penetrated to some distance into the rock (items 7, 19, 76, 77, and 78). Analysis and tests on sheet pile cells driven into sand indicated that failure by tilting due to overturning moment should occur long before the maximum sliding resistance is reached (item 55). Failure by sliding would occur if the resultant lateral force acts near the base of the cell, which is an unlikely event (item 47).

(2) However, sedimentary rock formations frequently contain clay seams between competent rock strata (item 31). Slickensides or a plane of weakness in a rock shelf may exist beneath the cell (items 7 and 77). Seams of pervious sand within the clay deposit, which may permit the development of excess hydrostatic pressure below the base of the cell, may also exist. Excess hydrostatic pressure reduces the effective stress and, subsequently, reduces shearing resistance to a very small value. This is a very common occurrence in alluvial soils (items 97 and 43).

(3) Drop of shear strength of clay shale to its residual strength due to removal of overburden pressure after excavation was observed by Bjerrum (item 8). Fetzer (item 30) reported a progressive failure of clay shale below Cannelton cofferdam.

(4) Hence, the possibility of a deep-seated failure along any weak seam below a cellular structure always exists before any other type of failure could occur. A detailed study of the subsurface below the design bottom of the cell and an adequate sliding analysis should, therefore, be conducted at the time of a cellular cofferdam design. If any potential for a sliding failure exists, adequate measures to prevent such failure should be incorporated in the cell design. Details of such investigation and preventive measures are discussed in subsequent paragraphs. Figure 4-7 illustrates how a deep-seated sliding failure may occur below a cell.

b. Study of Subsurface Conditions. The subsurface investigation should be extended to at least 15 to 20 feet below the design base level of the cell. Continuous sampling of soils or coring of rock should be performed in the presence of experienced geotechnical personnel to identify and locate any weak seam below the base. The presence of any cracks or joint pattern in the apparently competent rock mass below the base should be carefully investigated

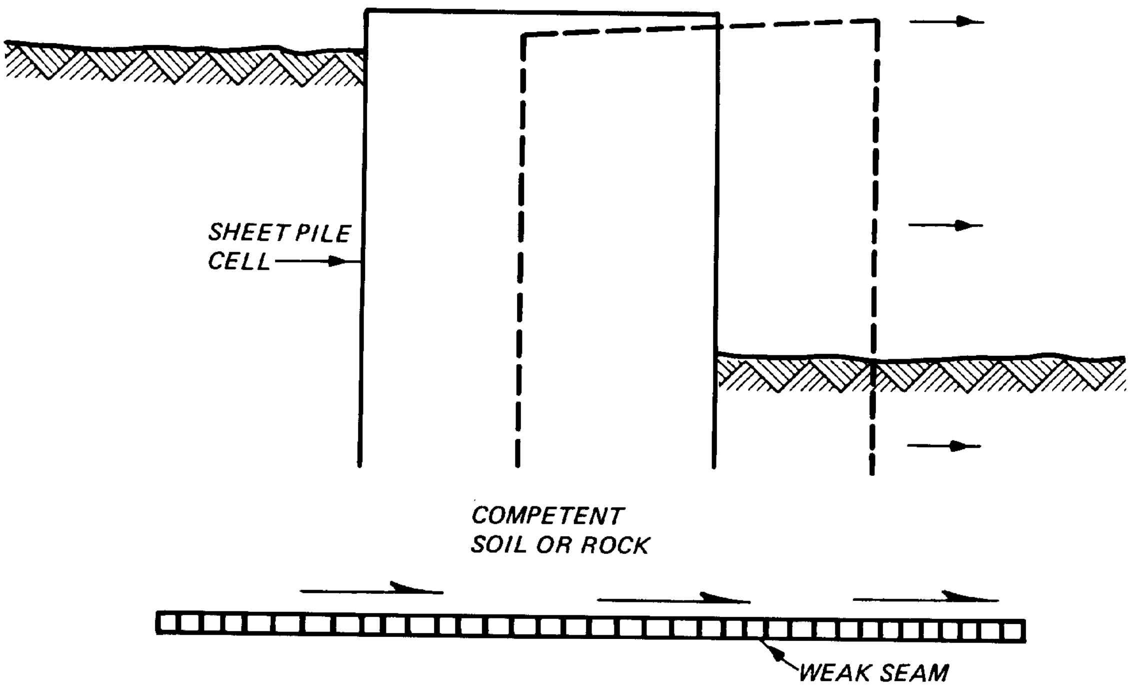

Figure 4-7. Deep-seated sliding failure

(item 13). If soft seams or presheared surfaces due to faulting are found, extremely low shear strengths approaching the residual strengths should be used in the analysis. Unless 100 percent core recovery is achieved, the presence of a soft or presheared seam should be assumed where the core is missing (item 30). Investigation of any weak seam below the cell should be extended to some distance beyond the inboard and the outboard sides of the cofferdam. This information will be useful in conducting sliding stability analyses.

c. Methods of Sliding Stability Analysis.

(1) Wedge Method.

(a) The FS against sliding failure along a weak seam below the cell can be determined by using the method of wedge analysis described in paragraph 4.9a. This method is discussed in detail in ETL 1110-2-256.

(b) For deep-seated sliding, a major portion of the failure mass slides along the weak seam. Hence, for each trial analysis, a large part of the failure surface should pass through the weak seam. The structural wedge is formed by the boundary of the cell section extended downward to the assumed failure surface. This wedge acts as the central block between the active and the passive wedge systems. Other assumptions including some simplifications made in the sliding analysis are the same as those discussed in paragraph 4-9a.

(c) The effects of cracks in the active wedge system and of seepage within the sliding mass including the uplift pressure beneath the structural wedge should be considered in the manner described in paragraph 4.9a(4). For each trial failure surface system, the minimum FS should be determined. The lowest value from all of these trials is likely to be the actual FS against sliding failure. A FS of 1.5 is adequate against a deep-seated sliding failure.

(2) Approximate Method. The approximate method may be used when the weak seam is located near the bottom of the sheet pile. The active and passive pressures acting on the sheet pile walls and the shearing resistance of the weak seam near the cell bottom are shown in Figure 4-8. Notation for Figure 4-8 follows:

B = equivalent width of cell, as discussed in paragraph 4-3

H_W = head of water on the outboard side

H_S = height of overburden on the outboard side

H_B = height of berm or overburden on the inboard side

W = weight of cell fill above the weak seam

p_W = hydrostatic pressure due to head, H_W

P_a = active earth pressure due to overburden of height, H_S

P_R = resultant of passive earth pressure due to buoyant weight of the berm + hydrostatic pressure due to height, H_B

R_S = lateral resistance along weak seam

Considering unit length of the cofferdam wall,

$$W = \frac{1}{2}(\gamma_c + \gamma_c')B(H_W - H_B) + \gamma_c' B H_B$$

where

γ_c = unit weight of cell fill

γ_c' = submerged unit weight of cell fill

$$R_S = W \tan \phi + Bc$$

where

ϕ = angle of shearing resistance

c = cohesion of materials in the weak seam

For clay, $\phi = 0$ and $c=c$

For sand, $\phi = \phi$ and $c=o$

$$P_W = 1/2\gamma_W H_W^2$$

where γ_W = unit weight of water

$$P_a = 1/2 K_a \gamma' H_S^2$$

where K_a = active earth pressure coefficient of overburden materials, and γ' = submerged unit weight of overburden materials.

$$P_R = P_P = 1/2\gamma_W H_B^2$$

where P_P = passive earth pressure of the saturated berm or overburden. Hence, the FS against sliding is

$$FS = \frac{W \tan \phi + B_c + P_R}{P_W + P_a}$$

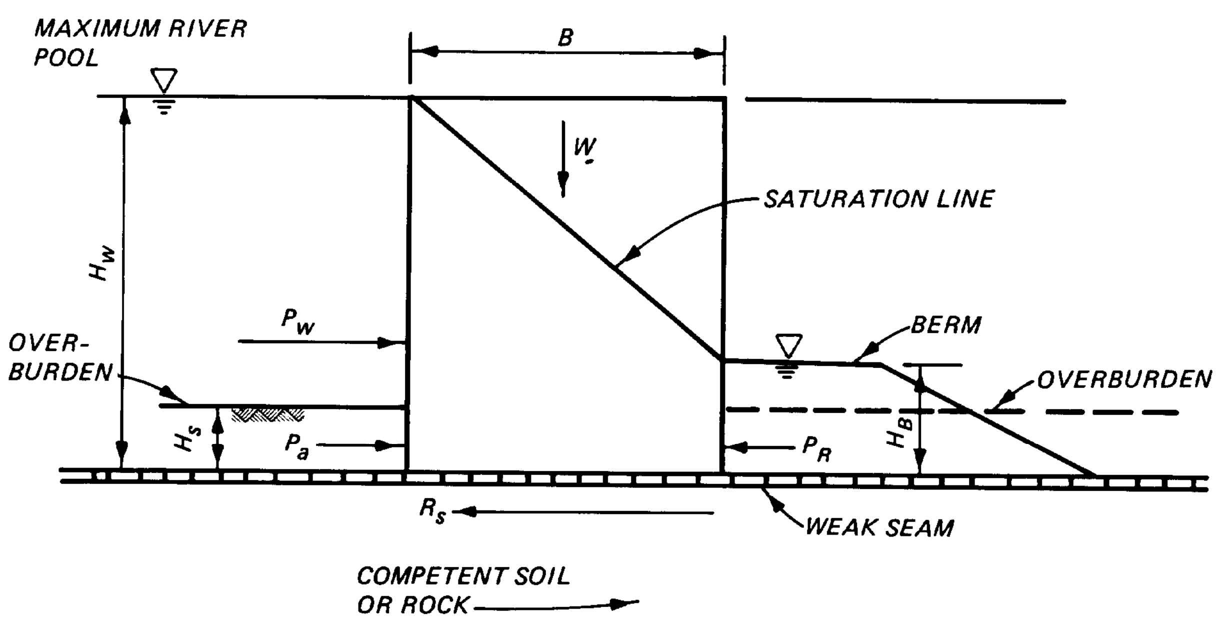

Figure 4-8. Sliding along weak seam near bottom of cell (approximate method)

(3) Culmann's Method. For a berm with combined horizontal and inclined surfaces, passive pressure should be calculated using Culmann's graphical method or any other suitable method. The lateral resistance at the interface of the berm and the weak seam should also be calculated. The smaller of the lateral resistance and the passive pressure should be considered in calculating the FS against sliding (item 27). For overburden with the horizontal surface to a great distance on the inboard side, the passive pressure can be calculated, using the passive earth pressure coefficient K_p. Since no effect of the weak seam is considered in the passive pressure calculation, the FS based on this passive pressure may be somewhat approximate. For more precise analysis, the wedge method described previously should be adopted.

d. Prevention of Sliding Failure. The potential for sliding stability failure can be considerably reduced by adopting the following measures.

(1) Seepage Control Below Cell. The extension of the sheet piles to considerably deeper levels below the cell will develop longer drainage paths and reduce the flow rate through the foundation materials, thereby decreasing the uplift pressure below the structural and the passive wedge systems and increasing the FS against sliding failure.

(2) Dissipation of Excess Hydrostatic Pressure. Excess hydrostatic pressure within a sand seam between clay strata below the cell will be dissipated quickly if adequate relief wells are installed within the seam. The shear strength of the sand seam will be increased and the potential for sliding failure along the seam will be reduced.

(3) Berm Construction on the Inboard Side. An inside berm will increase the passive resistance and will also aid in lengthening the seepage path discussed above only if impermeable berm is used. The berm should be constructed of free-draining sand and gravel so as to act as an inverted filter maintaining the free flow of pore water from the cell fill and the foundation materials. The increase in the passive resistance due to berm construction will improve the FS against sliding failure.

4-11. Bearing Capacity Analysis. The cells of a cofferdam must rest on a base of firm material that possesses the bearing capacity to sustain the weight of the filled cells (EM 1110-2-2906). Presence of weak soil beneath the cell may cause a bearing capacity failure of the entire structure inducing the cell to sink or rotate excessively (item 46). Figure 4-9 shows graphically bearing capacity failure of a cell supported on weak soil. The bearing capacity of rock is usually controlled by the defects in the rock structure rather than the strength alone. Defective and weak rock, such as some chalks, clay shales, friable sandstones, very porous limestones, and weathered, cavernous, or highly fractured rock may cause very large settlements under a relatively small load and reduce the load bearing capacity. Interbedding of hard (such as cemented sandstone) and very soft (such as claystone) layers may also cause bearing capacity problems (items 33 and 74). A cofferdam on rock

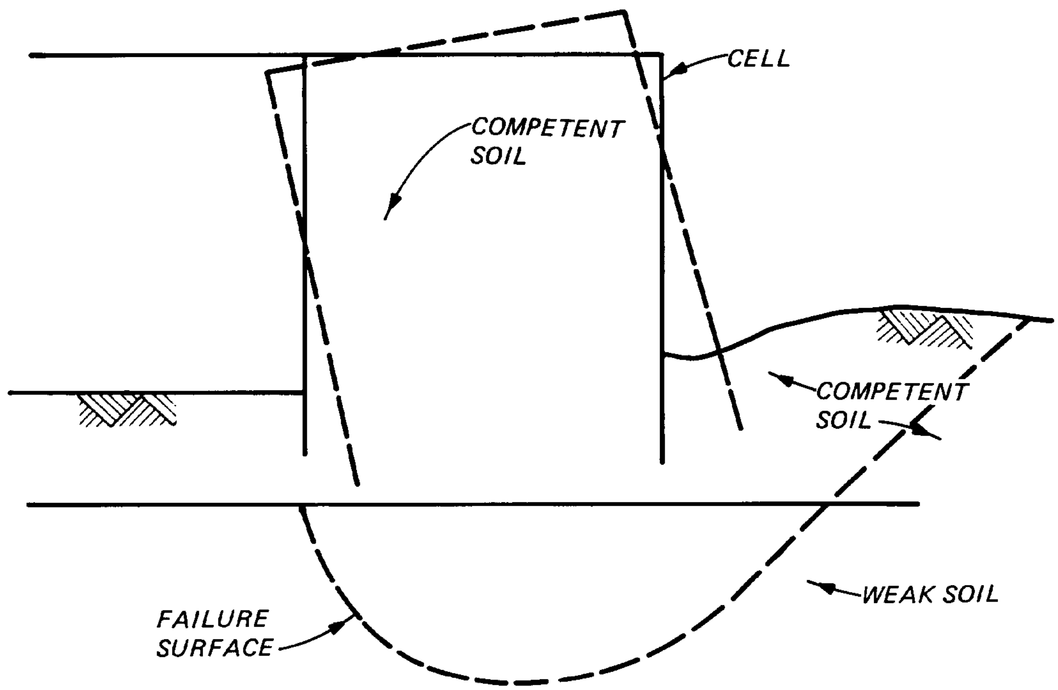

Figure 4-9. Bearing capacity failure

may not function properly due to shear failure of soil on the base of the rock or by deep-seated sliding along any weak seam within the rock. This aspect of the design has been discussed in paragraph 4-10. The methods of determining bearing capacity of soils and rock to support a sheet pile cellular structure are discussed below:

a. Bearing Capacity of Soils. The bearing capacity of granular soils is generally good if the penetration of the sheet piles into the overburden is adequate and seepage of water underneath the cell base is controlled. The seepage which reduces the shear strength of the soil on the inboard side of the cofferdam and thus reduces the bearing capacity can be controlled by using an adequate berm on the inboard side. Cellular structures on clay are not very common. The bearing capacity of clay depends on the consistency of the soils; the stiffer or harder the clay, the better the bearing capacity. For a good bearing capacity, the clay should be stiff to hard. However, even on relatively soft soils, cellular structures have been successfully constructed using heavy sand or rockfill berms (EM 1110-2-2906 and item 19). The bearing capacity of both cohesive and granular soils supporting cellular structures can be determined by Terzaghi's method of analysis (EM 1110-2-2906 and items 52, 27, and 85). However, the failure planes assumed for the development of the Terzaghi bearing capacity factors (item 80) do not appear to be as realistic as those developed specifically for cellular structures by Hansen (item 36). Hence, for bearing capacity investigation, the Hansen method of analysis should also be used (item 31). The investigation of failure along any weak stratum below the cell can be conducted by using the limit equilibrium analysis, as discussed previously in paragraph 4-9a. Methods of determining bearing capacity of soils are given below:

(1) Terzaghi Method, The ultimate bearing capacity is given by

$$q_f = 1/2\gamma B N_\gamma + cN_c + \gamma D_f N_q \qquad [4\text{-}1]$$

for strip loaded area and by

$$q_f = 0.6\gamma B N_\gamma + 1.3\ cN_c + \gamma D_f N_q \qquad [4\text{-}2]$$

for circular loaded area

where

γ = unit weight of soil around cell

B = equivalent cell width, as discussed in paragraph 4-3

N_c, N_q, N_γ = the Terzaghi bearing capacity factors (item 82) depending on the angle of shearing resistance, ϕ, of the soil

c = cohesion of soil

D_f = distance from the ground surface to the toe of the cell

The relevant tests to determine the strength parameters c and ϕ for the bearing capacity analysis are mentioned in EM 1110-2-1903. The FS against bearing capacity failure should be determined by the maximum pressure at the base of the cellular structures. Figure 4-10 shows the section of cofferdam of equivalent width, B , and subjected to a hydrostatic pressure of P_W , and active and passive pressures of P_a and P_R , respectively. The net overturning moment due to these lateral pressures is given by

$$M = 1/3(P_W H_W + P_a H_S - P_R H_B) \qquad [4\text{-}3]$$

where H_W , H_S , and H_B are as shown in Figure 4-10. The bearing soil is subjected to a uniform vertical compressive stress of W/B , where W is the weight of the cell fill. In addition, the soil is also subjected to a compressive stress developed due to the net overturning moment, M (equation [4-3]). This stress is equal to $6M/B^2$ (Figure 4-10). Hence, the FS against bearing capacity failure

$$FS = \frac{q_f}{\frac{W}{B} + \frac{6M}{B^2}}$$

where q_f can be determined from equation [4-1] or [4-2]. The FS for sand should not be less than 2 and for clay not less than 3, as given in Table 4-4.

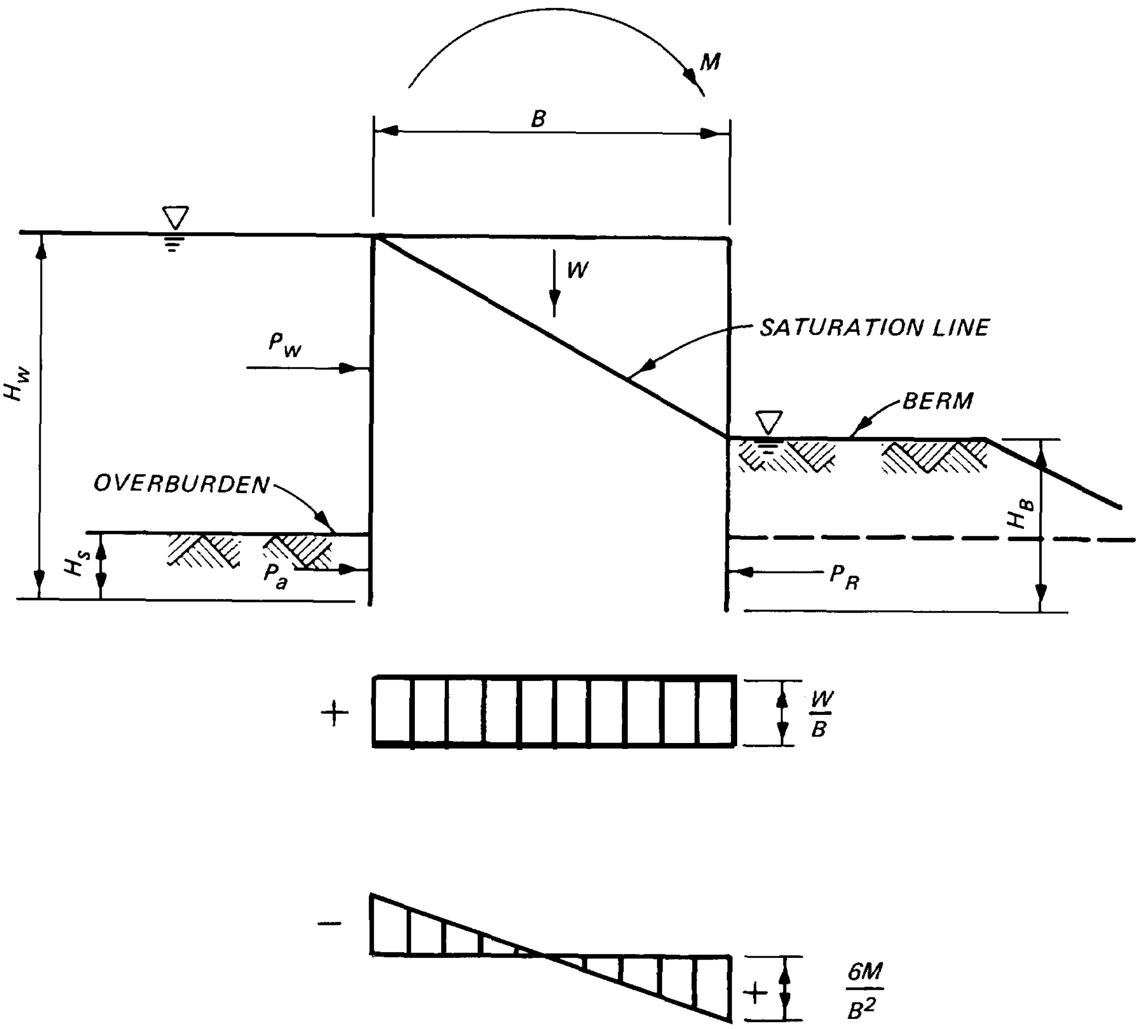

NET OVERTURNING MOMENT, $M = \frac{1}{3}\ (P_W H_W + P_a H_s - P_R\ H_B)$

Figure 4-10. Base soil pressure diagram

(2) Hansen Method. In the Hansen method of analysis, cells supported on soils are assumed to have surface of rupture within the cell fill (convex failure surface) or in the foundation soils below the cell (concave failure surface). Both possibilities must be investigated to determine the minimum FS. Details of this method of analysis have been discussed in paragraph 4-9c.

(3) Limit-equilibrium Method. This analysis is based on assumed plane failure surfaces which form the bases of the failure wedges. A FS is applied to the material strength parameters such that the failure wedges are in limiting equilibrium. The critical failure surface with the lowest safety factor is determined by trial wedge method. Details of this method of analysis have been discussed in paragraph 4-9. For the preliminary design of a cofferdam on soils, bearing capacity can be determined by the Terzaghi method. However, more rigorous analysis by the limit-equilibrium method should be applied for the final design. Hansen's method of analysis should be used to determine FS against a rotational failure of the cellular structure.

b. Bearing Capacity of Rock. The bearing capacity of rock is not readily determined by laboratory tests on specimens and mathematical analysis, since it is greatly dependent on the influence of nonhomogeneity and microscopic geologic defects on the behavior of rock under load (items 20, 33, and 74). The bearing capacity of homogeneous rock having a constant angle of internal friction ϕ and unconfined compressive strength q_u can be given as

$$q_f = q_u(N_\phi + 1) \qquad [4\text{-}4]$$

where $\tan^2\left(45^\circ + \frac{\phi}{2}\right)$. To allow for the possibility of unsound rock, a high value of the FS is generally adopted to determine allowable bearing pressure (item 11). A FS of 5 may be used to obtain this allowable pressure from equation [4-4]. Even with this FS, the allowable loads tend to be higher than the code values sampled in Table 4-1. In the absence of test data on rock samples, the somewhat conservative values in Table 4-1 may be used for preliminary design. When the rock is not homogeneous, the bearing capacity is controlled by the weakest condition and the defects present in the rock. For a rock mass having weak planes or fractures, direct shear tests conducted on presawn shear surfaces give lower bound residual shear strengths (item 18). A minimum of three specimens should be tested under different normal stresses to determine cohesion c and angle of internal friction ϕ. The ultimate bearing capacity can then be determined from equations [4-1] and [4-2] (Terzaghi method) by using the c and ϕ values obtained as described above. A FS of at least 3 should be adopted to determine allowable bearing pressure. Cells founded on rock should also be checked for rotational failure using Hansen's method as discussed in paragraph 4-9c. The minimum FS for this failure is 1.5, as given in Table 4-4.

4-12. Settlement Analysis. Generally two types of settlement can occur within a sheet pile cellular structure supported on compressible soils: the settlement of the cell fill and the settlement of the sheet piles. In some

Table 4-1

Allowable Bearing Pressures for Fresh Rock of Various Types (According to typical building codes, reduce values accordingly to account for weathering or unrepresentative fracturing.[1] Values are from Thorburn (item 83) and Woodward, Gardner, and Greer (item 96).)

Rock Type	Age	Location	Allowable Bearing Pressure (MPa) (1 MPa = 10.4 tsf)
Massively bedded limestone[2]		United Kingdom[3]	3.8
Dolomite	Late Paleozoic	Chicago	4.8
Dolomite	Late Paleozoic	Detroit	1.0-9.6
Limestone	Upper Paleozoic	Kansas City	0.5-5.8
Limestone	Upper Paleozoic	St. Louis	2.4-4.8
Mica schist	Precambrian	Washington	0.5-1.9
Mica schist	Precambrian	Philadelphia	2.9-3.8
Manhattan schist[4]	Precambrian	New York	5.8
Fordham gneiss[4]	Precambrian	New York	5.8
Schist and slate		United Kingdom[3]	0.5-1.2
Argillite	Precambrian	Cambridge, MA	0.5-1.2
Newark shale	Triassic	Philadelphia	0.5-1.2
Hard, cemented shale		United Kingdom[3]	1.9
Eagleford shale	Cretaceous	Dallas	0.6-1.9
Clay shale		United Kingdom[3]	1.0
Pierre shale	Cretaceous	Denver	1.0-2.9
Fox Hills sandstone	Tertiary	Denver	1.0-2.9
Solid chalk	Cretaceous	United Kingdom'	0.6
Austin chalk	Cretaceous	Dallas	1.4-4.8
Friable sandstone and claystone	Tertiary	Oakland	0.4-1.0
Friable sandstone (Pica formation)	Quaternary	Los Angeles	0.5-1.0

Notes:

1. When a range is given, it relates to usual rock conditions.
2. Thickness of beds greater than 1 m, joint spacing greater than 2 m; unconfined compressive strength greater than 7.7 MPa (for a 4-inch cube).
3. Institution of Civil Engineers Code of Practice 4.
4. Sound rock such that it rings when struck and does not disintegrate. Cracks are unweathered and open less than 1 cm.

areas settlement may also be caused by dewatering of the cofferdam area. Details of these settlements are discussed below:

a. Settlement of Cell Fill. The settlement of cell fill occurs under the self load of the fill placed within the cell. In normal construction procedure hydraulic fill is pumped into the cell in layers. Each increment of fill consolidates under its own weight and also under the load of the layers above it. Thus, the settlement of the lower fill has progressed by the time the last fill is placed (item 92). For granular fill, generally a majority of the settlement will have been accomplished soon after the fill placement. Hence, the postconstruction settlement of granular cell fill under its own weight is, generally, insignificant. No reliable method of settlement estimate of the cell fill during placement is currently available. This settlement is also of not much importance, since most of this settlement occurs before any additional vertical or lateral loads are applied to the cell. Any volume decrease of the cell fill due to settlement can always be compensated by placing additional fill in the cell before any other load is applied to the cell. Hence, no method of settlement estimate of the cell fill has been included herein. Cell fill can be densified by using vibratory probes to prevent seismically induced liquefaction, minimize settlements, and obtain necessary density of the cell fill required for cofferdam stability (items 65 and 72). However, generation of excess pore pressure in the cell fill and increase in interlock tension were reported during compaction by vibration. Hence, a pore pressure relief system should also be provided within the cell fill to limit excess pore pressures and to aid the compaction by draining water from the soil.

b. Settlement of Sheet Pile Cofferdam. A cellular cofferdam underlain by compressible soils below its base will undergo settlement due to the weights of the cell and berm fills. As observed by Terzaghi (item 81), if the compressible soils below the cofferdam continue to consolidate after the overturning moment has been applied, a relatively small moment suffices to produce a very unequal distribution of pressure at the base of the cell. This reduces the capacity of the cofferdam to carry overturning moment. Large postconstruction settlements of cellular wharf structure might damage the deck slab and interfere with all normal operations from the deck. A study of settlement behavior of a cellular structure is an essential part of the design; This settlement can be computed by the Terzaghi method (item 44) if the cell is underlain by clay, and by the Schmertmann (item 63) or Buisman (item 62) method if underlain by granular soils. Details of settlement analysis are discussed below:

(1) Settlement of Cofferdam on Clay. In a clay layer beneath the cofferdam, more settlement will occur below the center than will occur below the edges of the cofferdam because of larger stresses below the center than the edges under the uniform flexible load of the cell fill at the base of the cells. Additional unequal settlements will occur below the cells if berm or backfill is present on one side of the cofferdam. Figure 4-11 is a sketch of a cell on compressible soils underlain by rock.

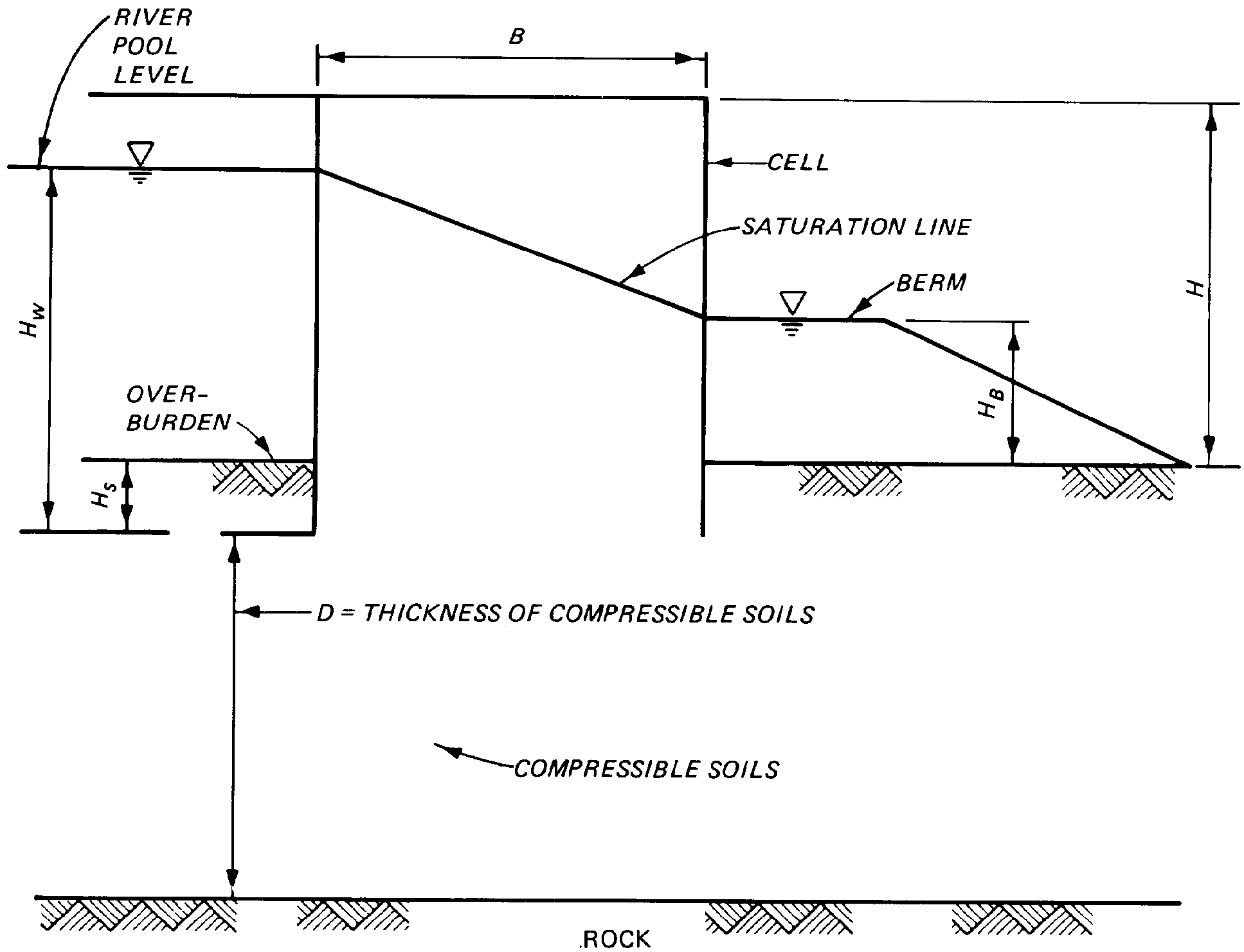

Figure 4-11. Cellular cofferdam on compressible soils

(a) Stresses Below Cell. Stresses at various levels below the center and the sides of the cellular cofferdam can be determined using Boussinesq's theory of stress distribution. The load due to cell fill in the cofferdam may be assumed to be a uniformly distributed contact pressure of a continuous footing of equivalent width B as defined in paragraph 4-3. For preliminary calculation, B may be taken as 0.85 times the cell diameter. If no rock is encountered at a relatively shallow depth, Fadum's chart in conjunction with the method of superposition of areas as given in EM 1110-2-1904 may be used to compute stresses in the compressible soil below any point in the cofferdam. If rock is encountered at a relatively shallow depth, stresses may be computed from the influence values given in the Sovinc (item 73) chart which includes correction for the finite thickness of the stressed medium (Figure 4-12). The trapezoidal section of the berm fill may be approximated to a rectangular section and the stresses may then be computed as described before. Alternately, the berm section may be divided into a rectangular and a triangular section. The stresses below the cell, due to these rectangular and triangular surface

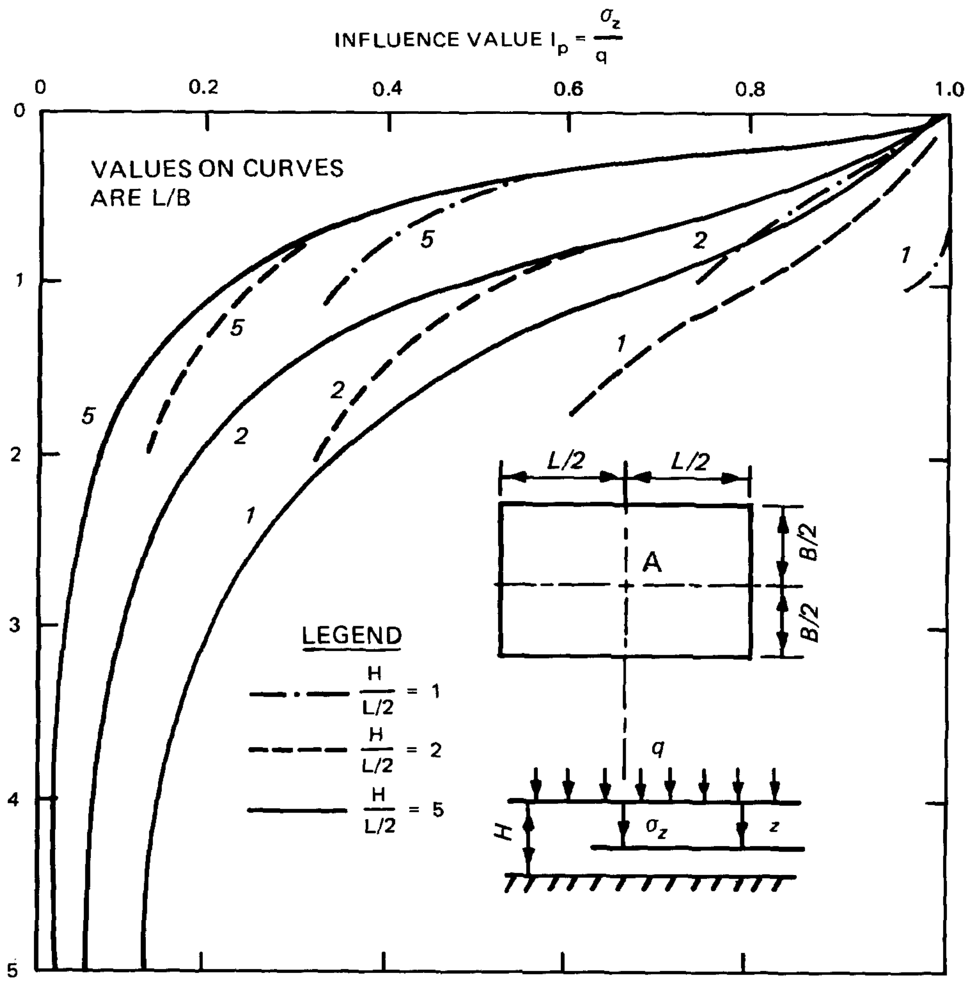

Figure 4-12. Influence value I_p for vertical stress σ_z at depth 2 below the center of a rectangular loaded area on a uniformly thick layer resting on a rigid base (item 73)

loadings, may then be calculated using vertical stress tables by Jumikis (item 41) or from appropriate charts given in textbooks. Stresses below surface can also be determined by using a suitable computer program, e.g. "Vertical Stresses Beneath Embankment and Footing Loadings," developed by US Army Engineer District, St. Paul, and available from WES.

(b) Settlement Computation. The clay stratum below the cell should be divided into several layers of smaller thicknesses. The stresses at the center of these layers should then be determined from the charts, tables, or by computer, as discussed above. The settlement of each layer can be given as

$$\Delta H_1 = \frac{H_1 C_c}{1 + e_o} \log_{10} \frac{\sigma_o + \Delta\sigma}{\sigma_o}$$

where

ΔH_1 = settlement of layer of thickness, H_1

C_c = compression index determined from the e versus log σ' curve

e = void ratio at any effective stress, σ'

e_o = initial void ratio

σ_o = effective overburden pressure

$\Delta\sigma$ = stress increment at the center of the layer due to cell and berm fills

Total settlement of clay below cell is

$$\Delta H = \sum \frac{HC_c}{1 + e_o} \log_{10} \frac{\sigma_o + \Delta\sigma}{\sigma_o} \qquad [4\text{-}5]$$

(2) Settlement of Cofferdam on Sand. The settlement of a foundation on sand occurs at a a very rapid rate following application of the load. For a cellular cofferdam on sand, a large part of the settlement of the foundation soils would occur during placement of fill inside the cells. As discussed before, the estimate of the total and differential settlements of a cellular structure is very important to examine any possibility of damage due to such settlements. The settlement of a structure on granular soils can be calculated by the Schmertmann or Buisman method, as described below.

(a) Schmertmann Method. This method is generally suitable for computing settlement below a rigid foundation, where the settlement is approximately uniform across the width of the foundation. However, the Schmertmann method has earlier been successfully used by Davisson and Salley (item 21) to predict average settlements of flexible foundations. Hence, the average settlement of a cellular cofferdam on granular soils may be determined using this method. To calculate the central and edge settlements below the flexible bottom of the cofferdam, the Buisman method with necessary correction suggested by Schmertmann may be used, as described later. The Schmertmann method utilizes the static cone penetration test values to estimate the elastic modulus of the soil layers. The settlement is calculated by integrating the strains, shown as follows:

$$S = \int_0^{\infty} \varepsilon_z \, dz = \Delta\sigma \int_0^{\infty} \left(\frac{I_z}{E_s}\right) dz$$

[4-6]

$$= C_1 C_2 \Delta\sigma \sum_1^n \left(\frac{I_z}{E_s}\right) \Delta z$$

where

S = total settlement

C_1 = foundation embedment correction factor

C_2 = correction factor for creep settlement

$\Delta\sigma$ = net foundation pressure increase at the base of the cell

$= \sigma - \sigma_o'$

σ = stress due to fill load at the base of the cofferdam

σ_o' = effective overburden pressure at the base of the cofferdam

I_z = strain influence factor at the center of each sublayer with constant q versus depth diagrams are shown in Figure 4-13(a)

q_c = static cone penetration resistance

E_s = modulus of elasticity of any sublayer

Δz = thickness of the sublayer

As recommended by Schmertmann, Hartman, and Brown (item 64), the peak value of the strain influence factor

$$I_{z\sigma} = 0.5 + 0.1 \left(\frac{\Delta\sigma}{\sigma_{y\sigma}'}\right)^{1/2}$$

where

$\sigma_{y\sigma}'$ = effective overburden pressure at depth B/2 or B , as explained in Figure 4-13(b) n = number of q_c sublayers to depth below footing which is equal to 2B (square or circular footing--axisymmetric case) or 4B (continuous footing--plane strain case).

B = equivalent width of the cofferdam, as explained before

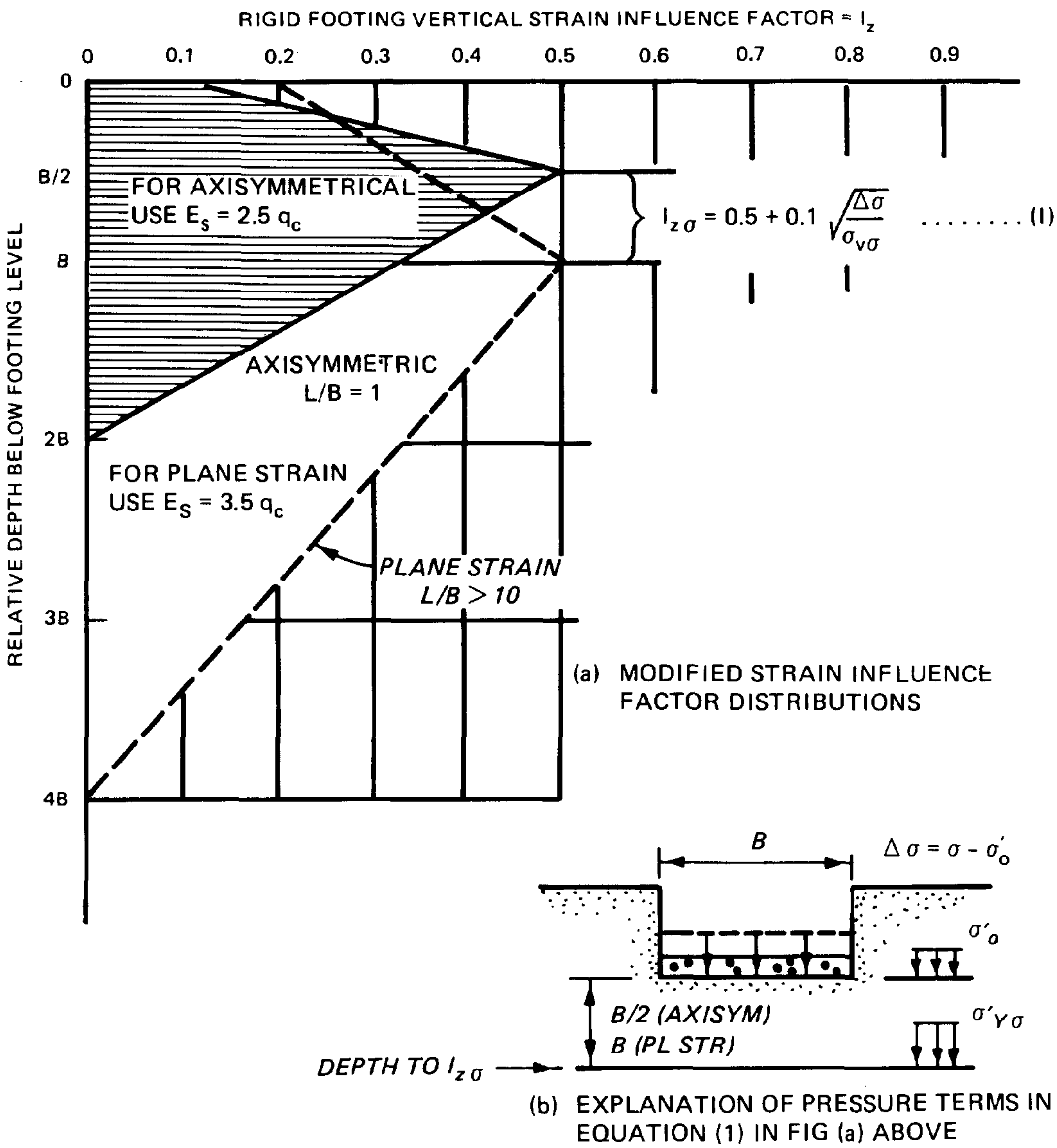

Figure 4-13. Recommended values for strain influence factor diagrams and matching E_s values (item 64)

The embedment correction factor

$$C_1 = 1 - 0.5\left(\frac{\sigma'_o}{\Delta\sigma}\right)$$

However, C_1 should equal or exceed 0.5. The correction for creep settlement

$$C_2 = 1 + 0.2 \log_{10}\left(\frac{t_{yr}}{0.1}\right)$$

where

t_{yr} = time in years from application of $\Delta\sigma$ on the foundation. The modulus of elasticity

$E_s = 2.5q_c$ for square or circular footing

and

$E_s = 3.5q_c$ for continuous footing

The following procedures should be adopted to compute settlement by the Schmertmann method:

- Obtain the static cone bearing capacity q_c for soils from the bottom of the cells to the significant depth which is equal to 2B for an axisymmetric case, or 4B for a plane strain case, e.g. for a cofferdam (L/B > 10), or to a boundary layer that can be assumed incompressible, whichever occurs first.

- Divide the soil depth, discussed above, into a succession of layers such that each layer has approximately a constant q_c .

- Superimpose the appropriate strain factor diagram shown in Figure 4-13 over the q_c - log discussed in step above. The strain influence factor diagram should be truncated at any rigid boundary layer if present within the significant depth discussed in step above. In this case, no vertical strains occur below this rigid boundary.

- Compute the total settlement, summing the settlements of individual layers using equation [4-6] and correcting for the embedment of the foundation and creep. In the expression for creep correction, C_2 , t_{yr} may be assumed as 5 years.

- For a cofferdam having 1 < L/B < 10 , the settlement should be computed for both axisymmetric and plane strain case, and then interpolated.

The settlement can also be calculated, but with somewhat reduced accuracy, using standard penetration test data (N) which should be converted to cone penetration resistance as suggested by Schmertmann (item 63). The ratios shown below are valid only for q_c values in tons per square foot.

Soil Type	q_c/N
Silts, sandy silts, slightly cohesive silt-sand mixture	2.0
Clean, fine to medium sands, and slightly silty sands	3.5
Coarse sand and sands with little gravel	5.0
Sandy gravel and gravel	6.0

(b) Buisman Method. As discussed before, the Schmertmann method is suitable for predicting settlement of a rigid foundation. The settlement computed by this method thus gives a somewhat average settlement of the cofferdam foundation which is essentially a flexible foundation. The Buisman method, like the Terzaghi method, determines settlement at any point within the soils below foundation. For the flexible foundation of the cofferdam, the stresses within the soils below the foundation can be determined using any of the suitable methods mentioned earlier for settlement on clay. The settlement of any granular stratum under these stresses can then be calculated using the Buisman expression:

$$\Delta H_1 = \frac{H_1}{C} \ln \frac{\sigma_o + \Delta\sigma}{\sigma_o}$$

where ΔH_1 , H_1 , σ_o, and $\Delta\sigma$ are same as explained in Schmertmann's method, and

$$C = \frac{1.5q_c}{\sigma_o}$$

Since the Buisman method highly overestimates the settlement, Schmertmann (item 63) suggested use of $2q_c$ instead of $1.5q_c$ as the elastic modulus of the soils in the above expression for C . Hence,

$$C = \frac{2q_c}{\sigma_o}$$

should be used to incorporate Schmertmann's correction in settlement calculation. Substituting this value of C in the settlement expression on the preceeding page

$$\Delta H_1 = \frac{H_1 \sigma_o}{2q_c} \times 2.303 \log_{10} \frac{\sigma_o + \Delta\sigma}{\sigma_o}$$

$$= \frac{1.151 \sigma_o H}{q_c} \times \log_{10} \frac{\sigma_o + \Delta\sigma}{\sigma_o}$$

Hence, total settlement at the point under consideration is given by

$$\Delta H = 1.151 \sum \frac{\sigma_o H}{q_c} \log_{10} \frac{\sigma_o + \Delta\sigma}{\sigma_o} \qquad [4\text{-}7]$$

This expression can be used to determine settlements at the center and the edges of the cofferdam to examine any possibility of the failure of the cofferdam due to excessive tilting under the loads of the cell fill, berm, or backfill.

c. Settlement Due to Dewatering of Cofferdam Area. Dewatering may cause drawdown of water levels within soil layers below existing structures or utility lines in the vicinity of the cofferdam area. This drawdown increases the effective weight of the soil layers previously submerged. Drawdown of water levels below the dredge level increases the effective stress in soils below the base of the cell. This increase in effective stress causes settlements of compressible soils underneath the structures within the drawdown zone (item 45). An estimate of these settlements is possible by using the methods discussed in paragraph 4-12b utilizing the drawdown depths to be determined by procedures described in Chapter 6.

4-13. <u>Seepage Analysis</u>. Generally two types of seepage are to be considered for designing a cellular cofferdam: seepage through the cell fill and foundation underseepage.

a. Seepage Through Cell Fill.

(1) The free water surface within the cell fill is to be estimated in order to check the stability of the assumed cell configuration. In general, the slope of the free water surface or saturation line may be assumed to be as shown in Figure 4-2. The effects on the saturation line during maximum pool, initial filling, and drawdown conditions have been discussed in paragraph 4-4. For simplifying seepage computations, a horizontal line may be chosen at an elevation representative of the average expected condition of saturation of the cell fill (item 86). However, adequate measures (e.g., providing weep holes and keeping free-draining quality of cell fill) should always be adopted to assure a reasonable low elevation of saturation.

(2) The zone of saturation within the cell fill is influenced by the following factors:

(a) Leakage of water into the cell through the outboard piles.

(b) Drainage of water from the cell through the inboard piles.

(c) Lower permeability than expected of the cell fill.

(d) Flood overtopping the outboard piles or wave splash.

(e) Possible leakage of water into the cell fill from any pipeline crossing the cells.

(3) Sometimes leakage through torn interlocks may occur if secondhand piles are used. For a permanent structure to retain high heads of water, new sheet piles in good condition should preferably be used (item 77).

(4) The hoop stresses due to cell fill are much smaller near the top than at the bottom of the cell. Hence, during the high flood period when the water rises near the top of the cell, water may leak into the cell through the top of the interlocks because of relaxation of the interlock joints. Therefore, the drainage facilities of the cell fill should always be well maintained.

(5) Floodgates should be provided such that the interior of the cofferdam can be flooded before the cells are overtopped by the rising water. Details of flooding the cofferdam are discussed in Chapter 6.

(6) Very hard driving in dense stratum or rock may open the sheet pile joints near the bottom of the cell causing leakage of water into the cell. If subsurface investigation indicates presence of such stratum, limitations regarding hard driving of sheet piles should be included in the contract specifications.

b. Foundation Underseepage. Cofferdams are primarily used for dewatering of construction areas and must sometimes withstand very high differential heads of water. If the cofferdam is supported on sand, seepage of water from the upstream to the downstream sides will occur through the sand stratum underneath the sheet piles due to the differential heads. Foundation problems, because of this seepage, have been discussed in EM 1110-2-2906 and various other publications (items 31, 52, and 81). Major problems associated with seepage below a sheet pile cellular structure are:

- Formation of pipe, boils, or heave of the soil mass in front of the toe because of the exit gradient exceeding the critical hydraulic gradient. Boils and heave will considerably lower the bearing capacity of the soil resulting in toe failure of the cell. Piping causes loss of materials underneath the cell foundation and may cause excessive settlement and eventual sinking of the cell.

- Upward seepage forces at the toe may excessively reduce the passive resistance of the soil. This loss of lateral resistance may cause sliding failure of the cell.

- Seepage forces acting on the soils at the inboard face of the cell may increase the hoop stress excessively in the sheet piles (item 46). This may increase the possibility of interlock failure of the sheet piles and result in the loss of cell fill.

(1) Studies of seepage by flow nets. The possibilities of different types of failures due to seepage through granular soils can be studied by flow net analysis. The quantity by seepage into the excavation can also be computed from the flow net. This can be used in designing pumping requirements to maintain a dry construction area. A typical flow net under a cell on sand is shown in Figure 4-14. The permeability of sand can be determined by field method (e.g., pumping test) or indirect method (e.g., grain size distribution curves) (EM 1110-2-1901 and item 79). The flow net below the cell can be constructed using a graphical, trial sketching method, generally called the Forchheimer solution (item 79). For anisotropic soil conditions the flow net must be drawn on a transformed section which can be used to determine the quantity of seepage. However, to determine magnitude and direction of seepage forces this transformed section should be reconstructed on the natural section (item 16).

(2) Seepage Quantity. The quantity of seepage can easily be determined once the flow net is available. The total number of flow channels and the total number of equipotential drops along each channel can be counted on any flow net. These numbers are N_f and N_p, respectively. If h is the head causing flow (Figure 4-14), then the quantity of seepage under the unit length of the cofferdam in unit time can be given by

$$Q = \frac{N_f}{N_p} kh \qquad [4\text{-}8]$$

where k is the coefficient of permeability which can be determined by the pumping test or the indirect method mentioned before.

(3) Heaving and Boiling. The average hydraulic gradient for any element, such as an element e in Figure 4-14, can be determined by the equation

$$i = \frac{\Delta h}{\Delta L}$$

where Δh is the head loss between the two potential boundaries of the square element and ΔL is the average length of the flow path between these boundaries. For the element e which is at the discharge face, the gradient is termed as the exit gradient or the escape gradient. The seepage force F acting on a volume V of an element is given by

$$F = i\gamma_w V \qquad [4\text{-}9]$$

where γ_w is the unit weight of the water. The direction of this force is approximately along the average direction of flow through the element. Heaving and subsequent piping failures can be expected to occur at the downstream side when the uplift forces of seepage exceed the downward forces due to the submerged weight of the soil. For sand, the submerged unit weight is very close to the unit weight of water. Hence, at the point of heaving, from equation [4-8], the hydraulic gradient becomes approximately equal to 1. This hydraulic gradient is termed as "critical hydraulic gradient i_c." For clean sand, exit gradients between 0.5 and 0.75 will cause unstable conditions for men and equipment (item 52). To provide security against piping failures, exit gradients should not exceed 0.30 to 0.40. High values of the hydraulic gradient near the toe of the cell greatly reduce the effective weight of the sand near the toe and decrease the passive resistance of the soils. This will increase the possibility of sliding failures of cofferdams.

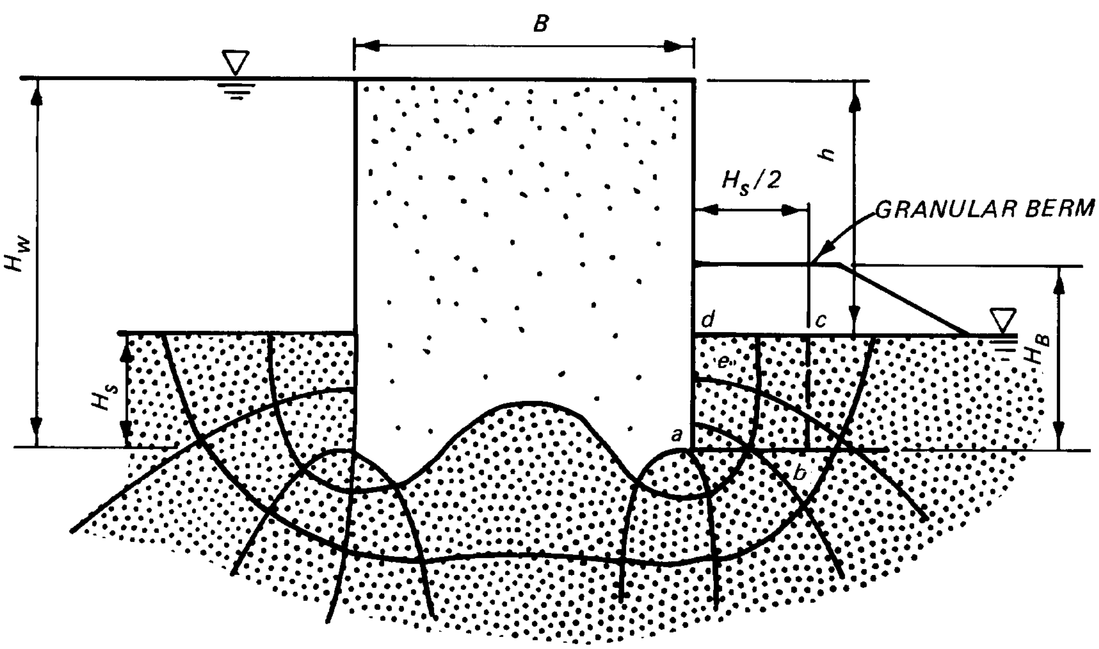

Figure 4-14. Partial flow net beneath a cell on sand

(4) Factor of Safety Against Piping Failure. It was observed from model tests that the heaving due to piping failure extends laterally from the downstream sheet pile surface to a distance equal to half the depth of sheet pile penetration (item 82). Figure 4-14 shows the prism 'abcd' subjected to seepage force causing piping failure. The distribution of the excess hydrostatic pressure at the base of the prism can be calculated from the flow net. If U is the excess hydrostatic force acting per unit length of the prism, then the FS against piping can be given by

$$FS = \frac{W'}{U} \qquad [4\text{-}10]$$

where W' is the submerged weight of the prism of unit length. To avoid any unstable condition of the downstream surface, a FS of at least 1.5 should be provided against piping failure. If the FS is less, adequate seepage control as discussed below should be done.

c. Control of Seepage. The following methods may be adopted to prevent seepage problems:

(1) Penetration of Sheet Piles to Deeper Levels. The penetration of sheet piles deep into the sand stratum below the dredgeline will increase the length of the percolation path that the water must travel to flow from the upper to the lower pool under the cofferdam (EM 1110-2-2906, items 52, 81, and. 94). The exit gradient to be determined from the new flow net can be lowered to an acceptable value of 0.3 to 0.4, as discussed before, by adequately increasing the penetration depth of the sheet piles. The excess hydrostatic force U acting on prism abcd (Figure 4-14) will also be reduced to yield a higher value of the FS as given by equation [4-10]. Terzaghi recommends a penetration depth equal to (2/3)H to reduce hydraulic gradients at critical locations, where H is the upstream head of water. However, critical hydraulic gradients should always be checked by actual flow net analysis.

(2) Providing Berm on the Downstream Surface. Deeper penetration of sheet piles in some cases may be uneconomical and impractical. A pervious berm can then be used on the downstream side to increase the FS against piping failures. The berm being more permeable than the protected soil will not have any influence on the flow net, but will counteract the vertical component of the seepage force. If the added weight of this berm acting as inverted filter is W , then the new FS according to equation [4-10] will be

$$FS = \frac{W + W'}{U}$$

(3) Increasing the Width of Cofferdam. The equivalent width of the cofferdam can be increased by using larger diameter cells. This will increase the percolation path of water under the cell from the outboard to the inboard sides. Adequate design may completely eliminate the necessity of berm on the downstream side. This may be very convenient for construction but is very expensive.

(4) Installation of Pressure Relief Systems. The exit gradient can also be reduced using adequate pressure relief systems that will lower the artesian head below the bottom of excavation to control upward seepage force (item 48). The relief wells act as controlled artificial springs that prevent boiling of soil (EM 1110-2-1905). If the discharge required to produce head reduction is not excessive, a wellpoint system can be effectively used. To relieve excess hydrostatic pressure in deep strata, a deep well system can be used. The well

can be pumped individually by turbine pumps or connected to a collector pipe with a centrifugal wellpoint pump system. Details of design of the relief well system have been discussed by Mansur and Kaufman and in EM 1110-2-1905. Details of dewatering are also included in Chapter 6 of this manual.

4-14. Internal Cell Stability.

a. Pile Interlock Tension. A cell must be stable against bursting pressure, i.e., the pressure exerted against the sheets by the fill inside the cell must not exceed the allowable interlock tension. The FS against excessive interlock tension is defined as the ratio of the interlock strength as guaranteed by the manufacturer to the maximum computed interlock tension. The interlock tension developed in a cell is a function of the internal cell pressure. The internal horizontal pressure p at any depth in the cell fill is the sum of the earth and water pressures. The earth pressure is equal to the effective weight of the cell fill above that depth times the coefficient of horizontal earth pressure K . This coefficient should ideally vary with the loading condition and the location within the cell; however, the actual variation is erratic and impossible to predict. It is recommended that a coefficient in the range of $1.2K_a$ to $1.6K_a$ is the coefficient of active earth pressure. The coefficient is dependent upon the type of cell fill material and the method of placement. See Table 4-2 for recommended values.

Table 4-2

Coefficients of Internal Pressure

Method of Placement	Type of Material: Crushed Stone	Coarse Sand and Gravel	Fine Sand	Silty Sand and Gravel	Clayey Sand and Gravel
Hydraulic dredge	$1.4K_a$		$1.5K_a$		$1.6K_a$
Placed dry and sluiced		$1.4K_a$		$1.5K_a$	
Wet clammed	$1.3K_a$		$1.4K_a$		$1.5K_a$
Dry material placed in dry		$1.3K_a$		$1.4K_a$	
Dumped through water	$1.2K_a$		$1.3K_a$		$1.4K_a$

Interlock tension is also proportional to the radius of the cell. The maximum interlock tension in the main cell is given by

$$t = pr$$

where

p = maximum inboard sheeting pressure

r = radius

The interlock tension at the connections between the main cells and the connecting arcs is increased due to the pull of the connecting arcs, as illustrated in Figure 4-15, and can be approximated by

$$t_{max} = pL \sec$$

where

t_{max} = interlock tension at connection

p = as previously defined

L = as shown in Figure 4-15

It must be emphasized that the above equation is an approximation since it does not take into account the bending stresses in the connection sheet pile produced by the tensile force in the sheet piles of the adjacent cell. Consequently, for critical structures, special analyses such as finite element should be used to determine interlock tension at the connections. In computing the maximum interlock tension, the location of the maximum unit horizontal

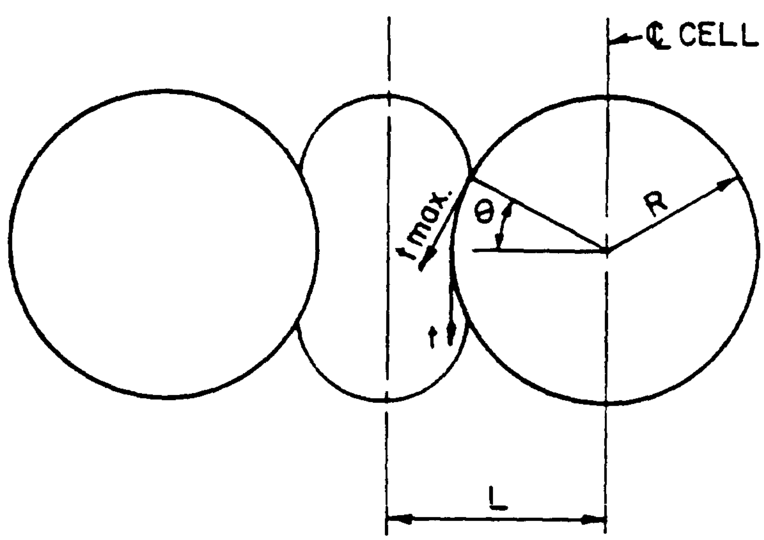

Figure 4-15. Interlock stress at connection

pressure p should be assumed to occur at a point one fourth of the height of the cell above the level at which cell expansion is fully restrained. Full restraint can be assumed to be where the external passive forces, due to overburden or a berm, and hydrostatic forces equal the internal cell pressures. In this case, it is generally sufficiently accurate and conservative to assume the point of maximum pressure to be at the top of the overburden or berm. When there is no overburden or berm, full restraint can be assumed to be at top of rock if the piling is seated on and bites into the rock. Maximum pressure should be assumed to occur at the base of cells which are neither seated in rock nor fully restrained by overburden or berm. See Figure 4-16 for typical pressure distributions. As stated previously, future changes in the depth of overburden, removal of berms, changes in saturation level in the cell fill, rate of dewatering, etc., must be anticipated when determining the maximum interlock tension.

b. Interlock Tension. In order to minimize interlock tension, the following details should be considered:

(1) Adequate weep holes should be provided on the interior sides of the cells in cofferdams to reduce the degree of saturation of the cell fill. The weep holes should be adequately maintained during the life of the cofferdam.

(2) Interlock tension failure has often occurred immediately after filling of the cells and can usually be traced to driving the sheets out of interlock. This results from driving through excessive overburden or striking boulders in the overburden. Overburden through which the piling must be driven should be limited to 30 feet. If the overburden exceeds this depth, consideration should be given to removing the excess prior to pile driving. The degree to which boulders may interfere with watertightness and driving of the cells can be estimated after a complete foundation exploration program.

(3) In an effort to reduce the effect of the connecting arc pull on the main cells, wye connectors are preferable to tees since the radial component of the pull on the outstanding leg is less for arcs of equal radius.

(4) Pull on the outstanding leg of connector piles can be reduced by keeping the radius of the connecting arc as small as practicable. The arc radius should not exceed one half of the radius of the main cell.

(5) Since tees and wyes are subjected to high local bending stresses at the connection, strong ductile connections are essential. Welded connections do not always meet this requirement because neither the steel nor the fabrication procedure is controlled for weldability. Therefore all fabricated tees, wyes, and cross pieces <u>shall</u> utilize riveted connections. In addition, the piling section from which such connections are fabricated <u>shall</u> have a minimum web thickness of one-half inch.

(6) Only straight web pile sections <u>shall</u> be used for cells as the hoop-tension forces would tend to straighten arch webs, thus creating high bending stresses.

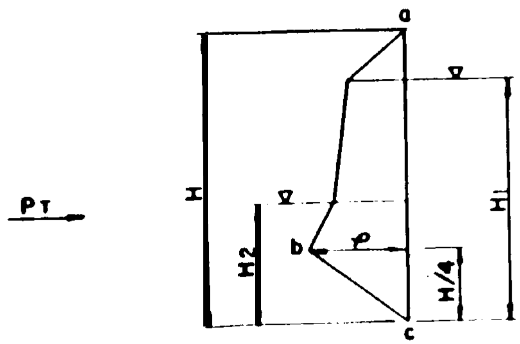

H1 = AVERAGE HEIGHT OF SATURATION LINE

H2 = HEIGHT OF SATURATION LINE AT INBOARD FACE

FIG. 4-16a PILING SEATED ON ROCK, NO OVERBURDEN OR BERM, ρ max@H/4

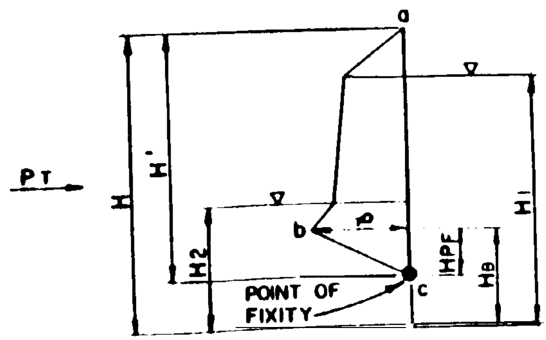

HB = HEIGHT OF BERM OR OVERBURDEN

HPF = DISTANCE FROM TOP OF BERM OR OVERBURDEN TO POINT OF FIXITY

H' = HEIGHT OF CELL ABOVE POINT OF FIXITY

FIG 4-16b PILING FULLY RESTRAINED BY EXTERNAL PASSIVE AND HYDROSTATIC FORCES, ρ max@H'/4 OR TOP OF BERM OR OVERBURDEN

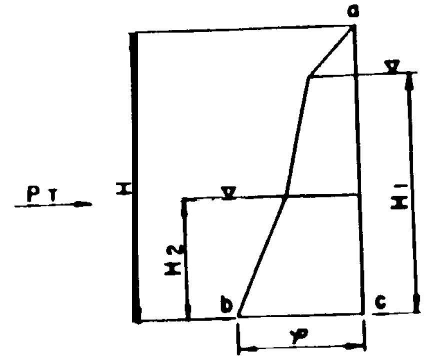

FIG 4-16c PILING NOT SEATED IN ROCK, ρ max@BASE OF CELL. PILING NOT FULLY RESTRAINED BY BERM OR OVERBURDEN, ρ max @ TOP OF BERM OR OVERBURDEN

Figure 4-16. Resultant interlock pressure and point of maximum horizontal pressure

(7) Used piling is often utilized with little regard to the manufacturer. Because of small differences in interlock configuration and dimensional tolerances, sheets from different manufacturers may not be compatible and may not develop the assumed interlock strength. Splices have been made without considering the dimensions of the sheets joined. Splicing two sheets that do not have exactly the same width can cause a stress concentration in the narrower sheet. Where previously used piling is employed, care should be taken to ensure that the sheets are gaged and will interlock and that the sheets are compatible for splicing.

c. Shear Failure Within the Cell (Resistance to Tilting). Tilting of cofferdam cells is resisted by both the vertical and horizontal shear resistance of the soil in the cell, to which the frictional resistance of the steel sheet piling is added. Vertical shear resistance is determined by the theory developed by Terzaghi (item 81). The horizontal shear resistance is determined by the theory proposed by Cummings (item 19). Both of these methods of analysis should be used independently to determine the adequacy of the cell to resist tilting. Additionally, tilting resistance of cells founded in overburden should be investigated by the theory proposed by Schroeder and Maitland (item 66).

(1) Vertical Shear Resistance. Excessive shear on a vertical plane through the center line of the cell is a possible mode of failure by tilting. For stability, the shearing resistance along this plane, together with the frictional resistance in the interlocks, must be equal to or greater than the shear due to the overturning forces. The frictional resistance in the interlocks must be included since shear failure cannot occur without simultaneous slippage in the interlocks. Figure 4-17a shows the assumed stress distribution on the base due to the net overturning moment. The total shearing force on the neutral plane at the center line of the cell is equal to the area of the triangle. Therefore

$$Q = \left(\frac{1}{2}\right)\left(\frac{B}{2}\right)\left(\frac{6M}{B^2}\right) = \frac{3M}{2B}$$

where

Q = total shearing force

M = net overturning moment

To prevent rupture, the shear resistance on the neutral plane must be equal to the shearing force Q on this plane. The shear resistance on the neutral plane is due to the lateral pressure of the cell fill and is equal to this pressure times the coefficient of internal friction of the cell fill. Thus, as illustrated in Figure 4-17b

$$Ps = \frac{1}{2}\gamma K(H - H_1)^2 + \gamma K(H - H_1)\ H_1 + \frac{1}{2}\gamma KH_1^2$$

where

Ps = total lateral pressure, per unit length of cofferdam, due to cell fill

= unit weight of cell fill above saturation line

= submerged unit weight of cell fill

$K = \dfrac{\cos^2\phi}{2 - \cos^2\phi}$, empirical coefficient of earth pressure as suggested by Kryine

ϕ = angle of internal friction of cell fill

The total center-line shear resistance per unit length of cofferdam is

$$Ss = Ps \tan \phi$$

where

Ss = total vertical shear resistance

$\tan \phi$ = coefficient of internal friction of cell fill

The frictional resistance in the sheet pile interlock is equal to the interlock tension times the coefficient of friction of steel on steel. The resistance against slippage per unit length is therefore

$$S_F = fP_T$$

where

S_F = frictional resistance against slippage

f = coefficient of friction of steel on steel at the interlock = 0.3

P_T = resultant interlock pressure (area abc on Figure 4-16)

The total shearing resistance S_T along the center line of the cell is then

$$S_T = Ss + S_F = Ps \tan \phi + fP_T$$

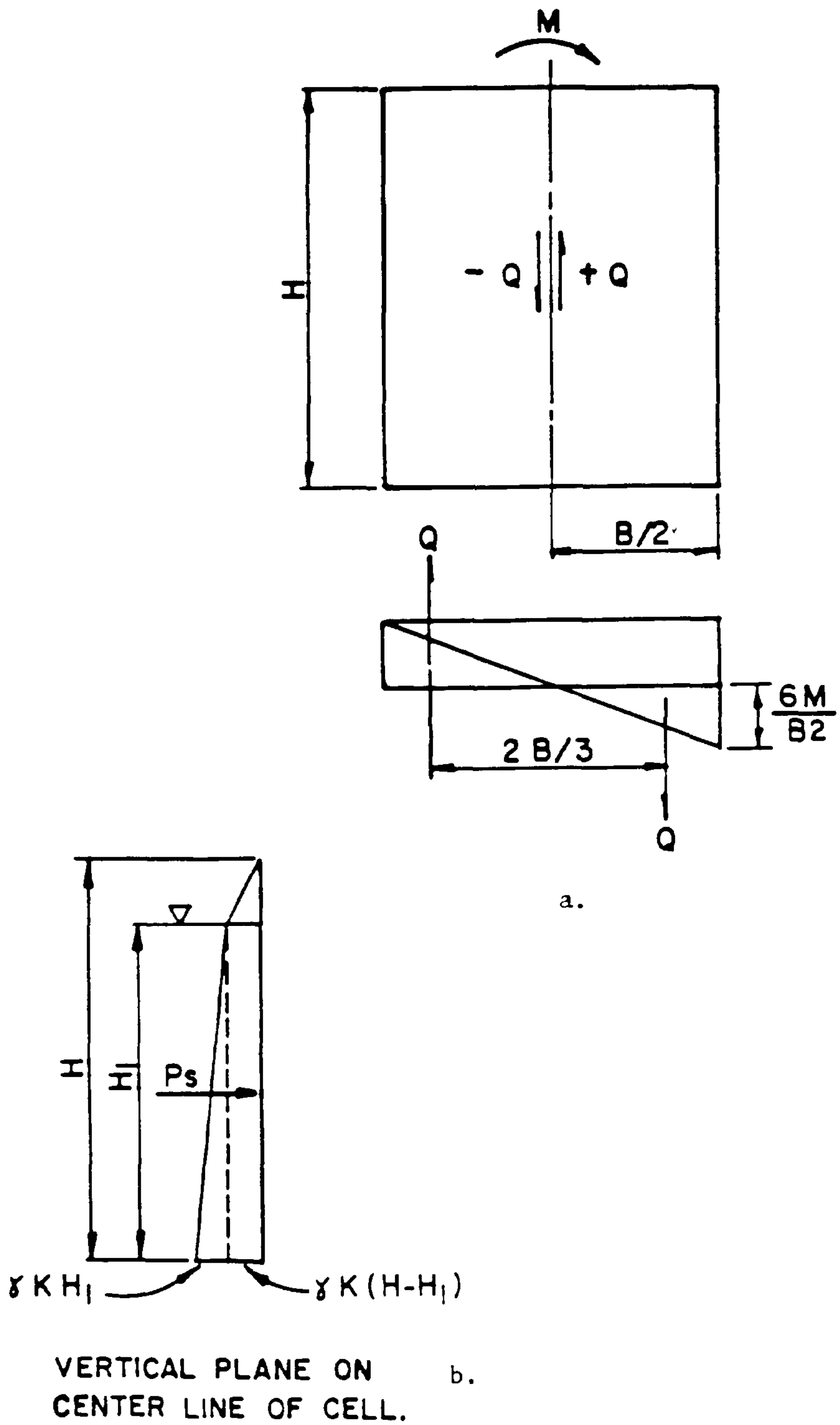

Figure 4-17. Vertical shear resistance, Terzaghi method

and the FS against tilting by vertical shear is thus

$$= \frac{S_T}{Q} = \frac{(Ps \tan \phi + fP_T)2B}{3M}$$

The foregoing is applicable to cells founded on rock, sand, or stiff clay. The determination of P_T is dependent upon whether the piling is seated on rock, the presence of a berm or overburden, and the degree of restraint provided thereby, as discussed previously. In the case of cells on soft to medium clay, a relatively small overturning moment will produce an unequal distribution of pressure on the base of the fill in the cell causing it to tilt. The stability of the cell is virtually independent of the strength of the cell fill since the shear resistance through vertical sections offered by the cell fill cannot be mobilized without overstressing the interlocks. Therefore, for cells on compressible soils, the shear resistance of the fill in the cells is neglected, and the factor of safety against a vertical shear failure is based on the moment resistance mobilized by interlock friction as follows:

$$FS = \frac{PRf\left(\frac{B}{L}\right)\left(\frac{L + 0.25B}{L + 0.50B}\right)}{M}$$

where

P = pressure difference on the inboard sheeting

R = radius

f = coefficient of interlock friction

B and L = as shown in Figure 4-1

M = net overturning moment

(2) Horizontal Shear Resistance. The stability of a cell against failure by tilting is also dependent on the horizontal shear resistance of the cell fill and on the resisting moment due to the frictional resistance of the pile interlock. This theory, as proposed by Cummings (item 19), is based on the premise that the cell fill will resist lateral distortion of the cell through the buildup of soil resistance to sliding on horizontal planes. This resistance will be developed in a triangle forming an angle ϕ to the horizontal as shown in Figure 4-18a. The triangle of soil will be in a passive pressure state and will be surcharged by the overlying fill. The magnitude of the resisting force F is

$$F = \gamma HB \tan \phi$$

where

$H = a + c$

$B = c/\tan \phi$

therefore

$$F = ac\gamma + c^2\gamma$$

The lateral force F is represented graphically by Figure 4-18b, the area of this diagram being equal to F. The total moment of resistance M_r about the base of the cell is

$$M_r = F_1\left(\frac{c}{2}\right) + F_2\left(\frac{c}{3}\right)$$

where

$F_1 = ac\gamma$

$F_2 = c^2\gamma$

therefore

$$M_r = \frac{ac^2\gamma}{2} + \frac{c^3\gamma}{3}$$

Interlock friction also provides shear resistance equal to the maximum interlock tension times the coefficient of interlock friction, with the maximum interlock tension being determined in accordance with the criteria set forth in paragraph 4-14a. Thus, the resisting moment M_f against tilting due to interlock tension is

$$M_f = P_T\, fB$$

where

P_T = area abc as shown in Figure 4-16

B and f = as previously defined

The FS against tilting due to horizontal shear is defined as

$$FS = \frac{M_r + M_f}{M_o}$$

where M_o = driving moment. Excessive tilting results from the use of weak cell fill; therefore, the fill should be well graded and free draining to the maximum extent possible. Further, since the shear resistance of the cell is

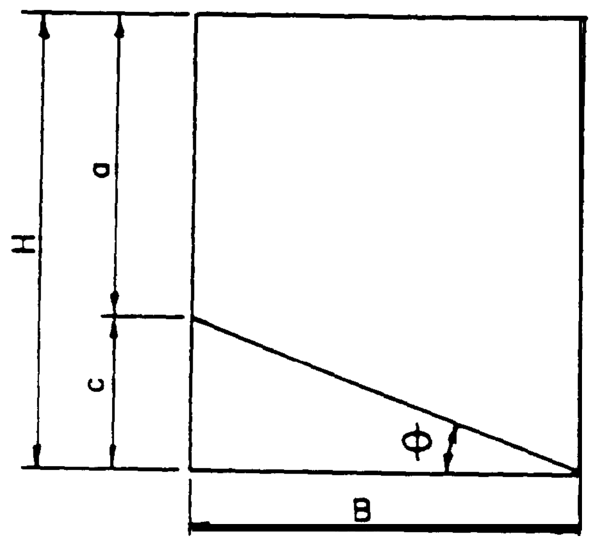

a.

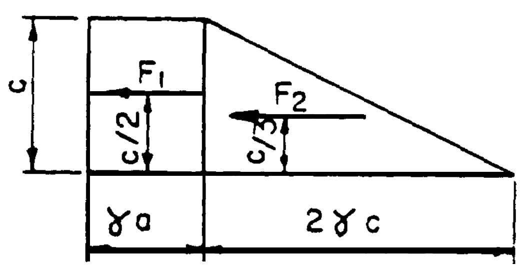

b.

Figure 4-18. Horizontal shear resistance, Cummings method

derived from the material in the lower portion of the cell, it may be necessary to excavate any weak material encountered in the overburden. Should the shear resistance of the cell fill material be inadequate to withstand the external forces, consideration should be given to the use of a berm to assist in stabilization of the cell. If a berm is used, the resisting moment due to the effective passive pressure of the berm should be included. Thus, the FS against tilting due to horizontal shear is

$$FS = \frac{M_r + M_f + P_R(H_B/3)}{M_o}$$

All variables are as previously defined.

(3) Vertical shear resistance (Schroeder-Maitland method, item 66). This design approach is a variation of the Terzaghi method of vertical shear resistance (see paragraph 4-14c(l)). It is particularly applicable to cells founded on sand or stiff to hard clay. The main premises, as determined from field and laboratory studies, are: the coefficient of lateral earth pressure K should be taken as 1 as a result of the compression the cell fill undergoes during the application of the overturning force; and the height of the cell over which vertical shear resistance is applied should extend from the top of the sheet piles on the cell center line to the point of fixity for the embedded portion of the sheets. Thus, as illustrated in Figure 4-19:

$$S_T = \frac{1}{2} \gamma K (H')^2 (\tan \phi + f)$$

where

S_T = total shearing resistance along the center line of the cell

K = coefficient of lateral earth pressure = 1.0

H' = height of cell over which vertical shear resistance is applied

γ, ϕ, and f = as previously defined

The point of fixity and the required depth of embedment, as determined by Matlock and Reese (item 58) for laterally loaded embedded piles, is 3.1T and >5T, respectively, where

$$T = \sqrt[5]{\frac{EI}{n_h}}$$

where

E = modulus of elasticity of the pile

I = moment of inertia of the pile

n_h = constant of horizontal subgrade reaction

Application of this method has the effect of satisfying the FS requirement against vertical shear failure with a smaller diameter cell than that required by the Terzaghi method. In installations where seepage resulting from an unbalanced head is not a critical consideration, i.e., a bulkhead installation as opposed to a cofferdam, the depth of embedment of the piling should be that required to provide passive resistance to translational failure rather than D = 2H/3 as recommended by Terzaghi. Sheet pile cells are flexible structures with a plane of fixity only a short distance below the dredgeline. In

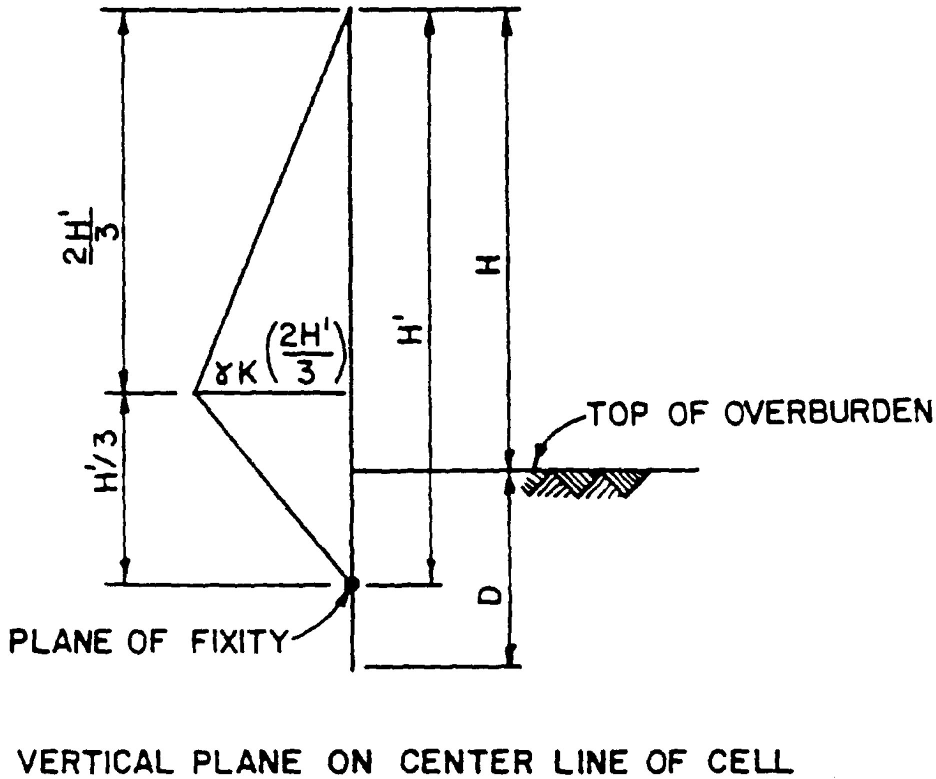

Figure 4-19. Vertical shear resistance Schroeder-Maitland method (item 66)

determining the depth of embedment, the plane of fixity should be determined by the analytical methods noted previously and the passive resistance available be calculated above this plane.

d. Pullout of Outboard Sheets. The depth of embedment of sheet piling is generally determined by the need to control seepage by increasing the flow path. However, the penetration must be sufficient to ensure stability with respect to pullout of the outboard piling due to tilting. The calculated overturning moments are applied to the sheet piles which are assumed to act as a rigid shell. Resistance to pullout is computed as the frictional or cohesive forces acting on the embedded length of piling. Thus

$$FS = \frac{Q_u}{Q_p}$$

where

Q_u = ultimate pullout capacity per linear foot of wall

Q_u clay = (Ca) (perimeter) (embedded length D)

Ca = adhesion

perimeter = interior and exterior surfaces of a l-foot-wide strip, i.e., 1 x 2 = 2 feet

D = embedded length

Q_u granular = $(1/2\ Ka\ \gamma e\ D^2 \tan \delta)$ (perimeter)

Ka = coefficient of active earth pressure by Coulomb

γe = effective unit weight of underlying soil

$\tan \delta$ = coefficient of friction for steel against underlying soil. See Table 4-3 for recommended values.

Q_p = average pile reaction due to overturning moment on outboard piling = $\dfrac{P_w H_w + P_a H_s - P_R H_B}{3B(1 + B/4L)}$, where all variables are as shown in Figure 4-5.

Table 4-3

Wall Friction

Steel Sheet Piles Against the Following Soils	tan δ
Clean gravel, gravel-sand mixtures, well-graded rock fill with spalls	0.40
Clean sand, silty sand-gravel mixture, single size hard rock	0.30
Silty sand, gravel or sand mixed with silt or clay	0.25
Fine sandy silt, nonplastic silt	0.20

e. Penetration of Inboard Sheets. The penetration of the sheet piles on the inboard side must be sufficient to prevent further penetration. The FS against sheet pile penetration is defined as the ratio of the shear resistance on both sides of the embedded portion of the piles on the unloaded side to the internal downward shear force on the unloaded side as follows:

$$FS = \frac{F_1}{M} (D)$$

where

$F_1 = P_T \tan \delta$

p_T = area abc as shown in Figure 4-16

$\tan \delta$ = coefficient of friction between steel sheet piling and cell fill

M = net overturning moment

D = embedded length

Section IV. Design Criteria

4-15. Factors of Safety. The required FS for the various potential failure modes described in paragraph 4-4 are listed in Table 4-4. As previously stated in Chapter 1 cofferdams are not classified as temporary structures, nor are the loads imposed upon them generally considered temporary as far as FS's are concerned. However, some loading conditions can be classed as temporary where failure would not result in loss of life, severe property damage, or loss of the navigation pool, e.g., initial dewatering of a cofferdam which does not maintain a navigation pool.

4-16. Steel Sheet Piling Specifications. Steel for sheet piling should conform to the requirements of the following American Society for Testing and Materials (ASTM) standards (item 4):

A328 Steel Sheet Piling

A572 High-Strength Low-Alloy Columbium Vanadium Steels of Structural Quality

A690 High-Strength Low-Alloy Steel H-Piles and Sheet Piling for Use in Marine Environments

A328 is the basic sheet piling specification and is satisfactory for most installations. A572 specifies high-strength sheet piling and is applicable for use in large diameter (>70 feet) cells where high interlock strength is required. A690 steel sheet piling provides greater corrosion resistance than other steels and should be considered for use in permanent structures in corrosive environments. The mechanical properties of the steel sheet pile grades are shown in Table 4-5. Cold-formed steel sheet piling is also available. Presently, there is no ASTM specification covering this piling. Although this piling has limited applicability, it may be used subject to the approval of Headquarters, US Army Corps of Engineers (CEEC-ED). An extruded

Table 4-4

Design Criteria--Factors of Safety

Failure Mode	Required Factor of Safety — Loading Condition: Normal	Temporary	Seismic
Sliding[1]	1.5	1.5	1.3
Overturning (gravity block)[1,2]	Inside Kern	Inside Kern	Inside Base
Rotation (Hansen)[2]	1.5	1.25	1.1
Deep seated sliding	1.5	1.5	1.3
Bearing capacity			
Sand	2.0	2.0	1.3
Clay	3.0	3.0	1.5
Seepage control			
Interlock tension[3]	2.0	1.5	1.3
Vertical shear resistance (Terzaghi)	1.5	1.25	1.1
Horizontal shear resistance (Cummings)	1.5	1.25	1.1
Vertical shear resistance (Schroeder-Maitland)[2]	1.5	1.25	1.1
Pullout of outboard sheets[2]	1.5	1.25	1.1
Penetration of inboard[2] sheets	1.5	1.25	1.1

Notes

1. These FS's/criteria are for cofferdams only. Refer to the appropriate engineer manual for the required FS for other installations or applications.

2. Design should not be based on these modes of failure, but rather these analyses should be employed as sensitivity checks only.

3. The FS against interlock tension failure should be applied to the interlock strength value guaranteed by the manufacturer for the particular grade of steel. The guaranteed value for used piling should be reduced as necessary depending upon the condition of the piling.

Table 4-5

Mechanical Properties

ASTM Grade	Minimum Yield Point, psi	Minimum Tensile Strength, psi	Interlock Strength, p1i.[1]
A328	38,500	70,000	16,000
A572(Gr. 50)	50,000	65,000	28,000
A690	50,000	70,000	28,000

Note

1. As guaranteed by the manufacturer.

wye, using A572, Grade 50 steel, is available on a limited basis. These wyes have a small cross section and are extremely flexible, thus creating handling and driving difficulties. As a result of this characteristic, together with their limited availability, the use of extruded wyes is not recommended.

4-17. Corrosion Mitigation. Permanent sheet pile structures located in polluted, brackish, or salt water should be protected against corrosion. A690 steel sheet piling, which offers greater corrosion resistance than A328 piling, should be considered for corrosive environments. A328 steel sheet piling with a protective coating in the splash zone, such as a coal-tar epoxy, should also be considered. For maximum protection, coatings can be applied to A690 piling.

Section V. Finite Element Method (FEM) for Analysis and Design

4-18. Background. The application of FEM analysis to date has been to develop its state of the art to the point where it can be used to refine existing design techniques and to analyze potential failure modes which cannot be checked by other methods. All studies so far have been made by researchers or engineers who are extremely familiar with the FEM techniques using specialized FEM programs for soil and structure modeling. The FEM analysis does not yet lend itself to application by typical design engineers working with currently available general-use programs. Due to FEM techniques currently being used for research applications, the information provided by this section will be limited to a review of available literature and methods used for analysis. Relatively little has been published concerning finite element analyses of cellular cofferdam structures. Kittisatra (item 42) was one of the first to apply FEM to cellular cofferdams by using a linear elastic axisymmetric model. Clough and Hansen (item 18) were the first to utilize FEM soil-structure interaction techniques in the analyses of cellular cofferdams. They developed a vertical slice model which was used to analyze the US Army Corps of Engineers Willow Island Cofferdam. Later, Dr. Clough used this model along with two others, axisymmetric and horizontal slice models, to analyze the US Army

Corps of Engineers Lock and Dam No. 26 (Replacement) for Shannon and Wilson, Inc. (item 69).

4-19. Finite Element Cofferdam Models. Due to the difficulty of early investigations to define exactly the forces involved with interaction between sheet piles, soils, and the foundation, empirical methods for design of cellular cofferdams have been adopted over the years. Recent studies of the finite element method have shown that two dimensional models of a circular cell cofferdam can, with a few basic assumptions, fairly accurately determine interactive forces between cell elements. A finite element program must contain four special capabilities: nonlinear stress-strain material behavior, slip elements, construction simulation, and orthotropic shell response. Soils are known to have a complex stress-strain response. The stress-strain behavior of a sand is characterized by a family of nonlinear curves in loading and a second family of essentially linear responses in unloading-reloading which depends upon the confining stress level. Currently only one set of variations of the finite element program "Soil-Struct," developed by Dr. Wayne Clough, contains all of the special capabilities needed for soil-cofferdam interaction modeling. This program is described in item 69. Three types of finite element models have been performed on cellular cofferdams as described below:

a. Vertical Slice Analysis. The first and most common model is a "Vertical Slice" analysis through the center of a circular cell from upstream to downstream side. This model has been used with good results by Dr. Clough for Shannon and Wilson, Inc. to simulate analysis of all stages and construction for cells resting on soil. A vertical slice model was also used in the report on Willow Island Cofferdam by Clough and Hansen (item 18), in which cells founded on rock with an underlying soft clay seam are analyzed. Figures 4-20 and 4-21 show this particular finite element model.

b. Axisymmetric Cell Analysis. The second model type is a vertical slice cut through the cell from center line out called an "Axisymmetric Model," shown in Figures 4-22 and 4-23. This analysis technique computes stresses and deflections of the sheet piling, cell fill, and foundation during cell filling. This model is not useful for other construction steps due to the assumption of axisymmetric loading. Axisymmetric Model Analysis is used by Dr. Clough for Shannon and Wilson, Inc. in their analysis of the Lock and Dam 26 (Replacement). Both this and the vertical slice types of models are analyzed with interface slip elements between sheets and cell fill, and on any planes in the foundation where slippage could occur.

c. Horizontal Slice Analysis. The third analysis model, Figures 4-24 and 4-25, is a "Horizontal Slice" including from center-line main cell to center line of arc cell and from outermost edge to center line of cofferdam. This horizontal slice model may be used at many different elevations in the cell to obtain a better analysis of interlock tension and sheet pile stresses. Since a symmetrical loading is assumed on the structure, this analysis technique can only be used for analyzing forces due to cell filling.

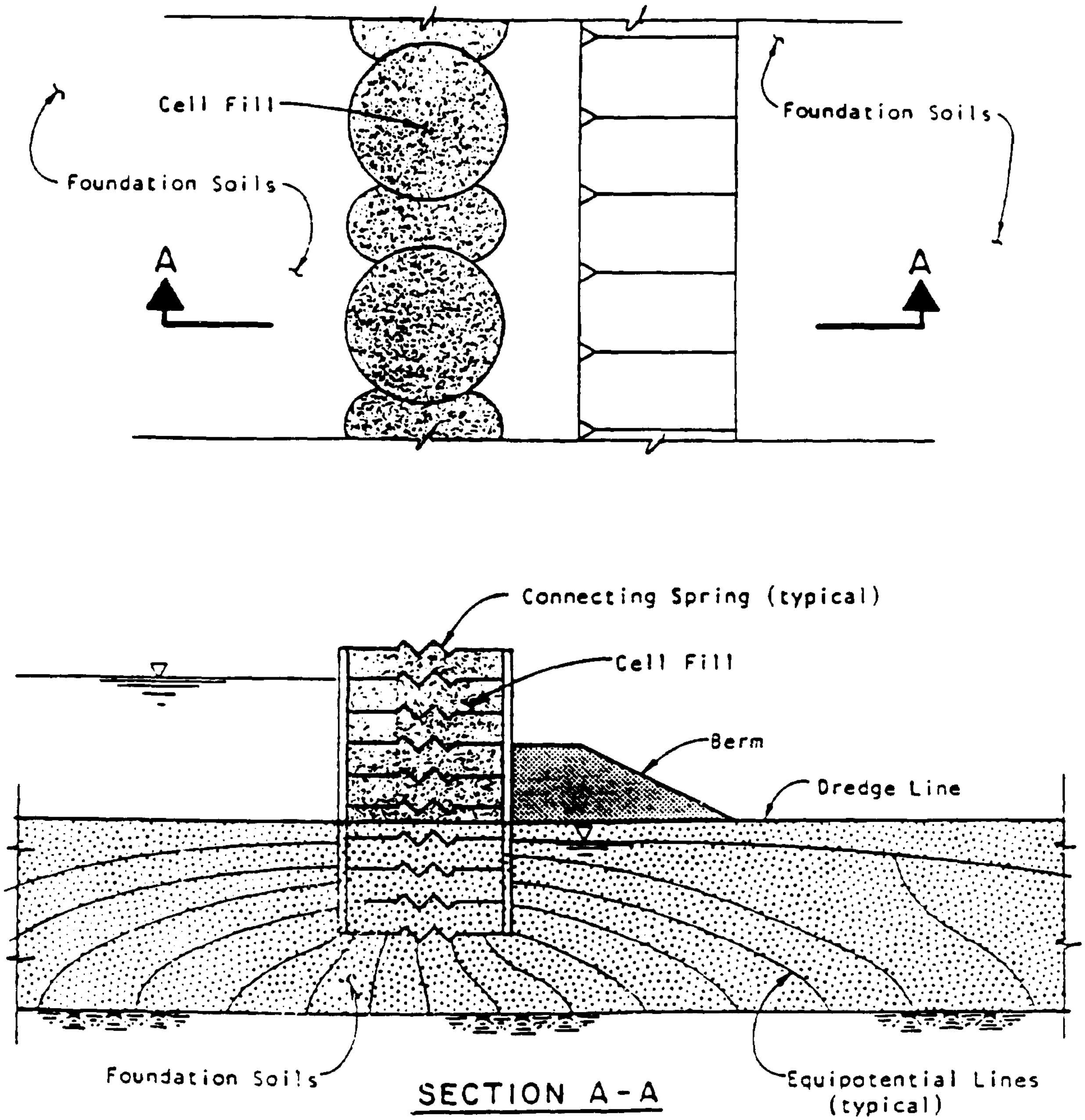

Figure 4-20. Schematic drawing, vertical slice model

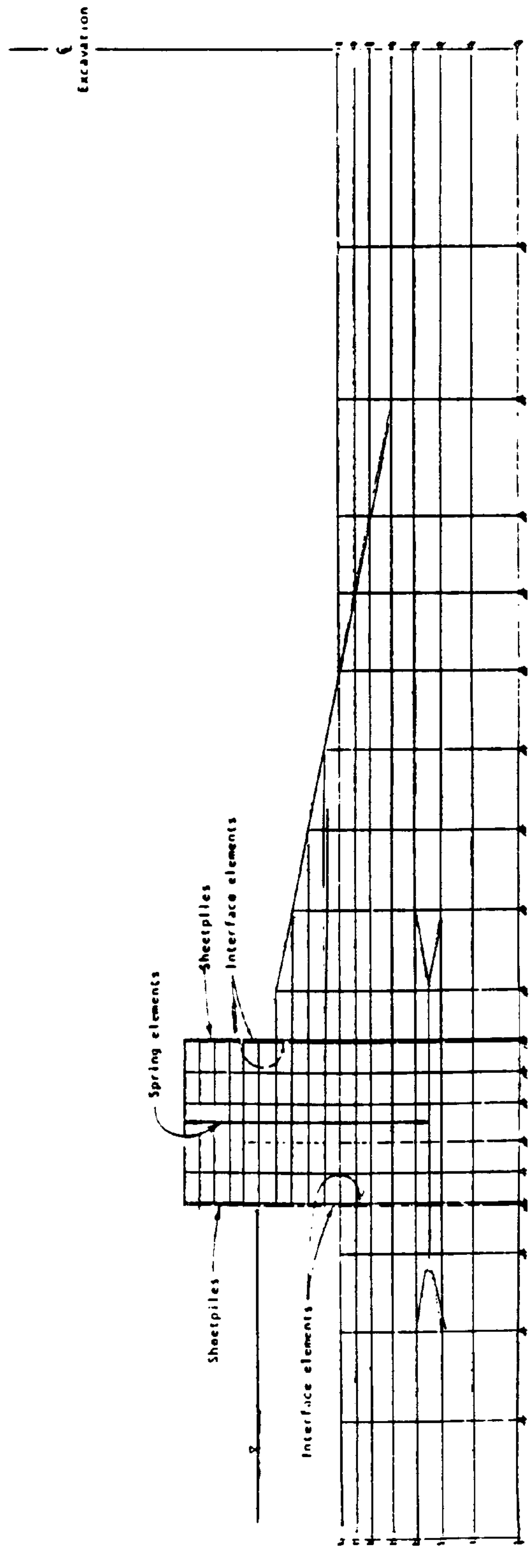

Figure 4-21. Vertical slice analysis, finite element mesh

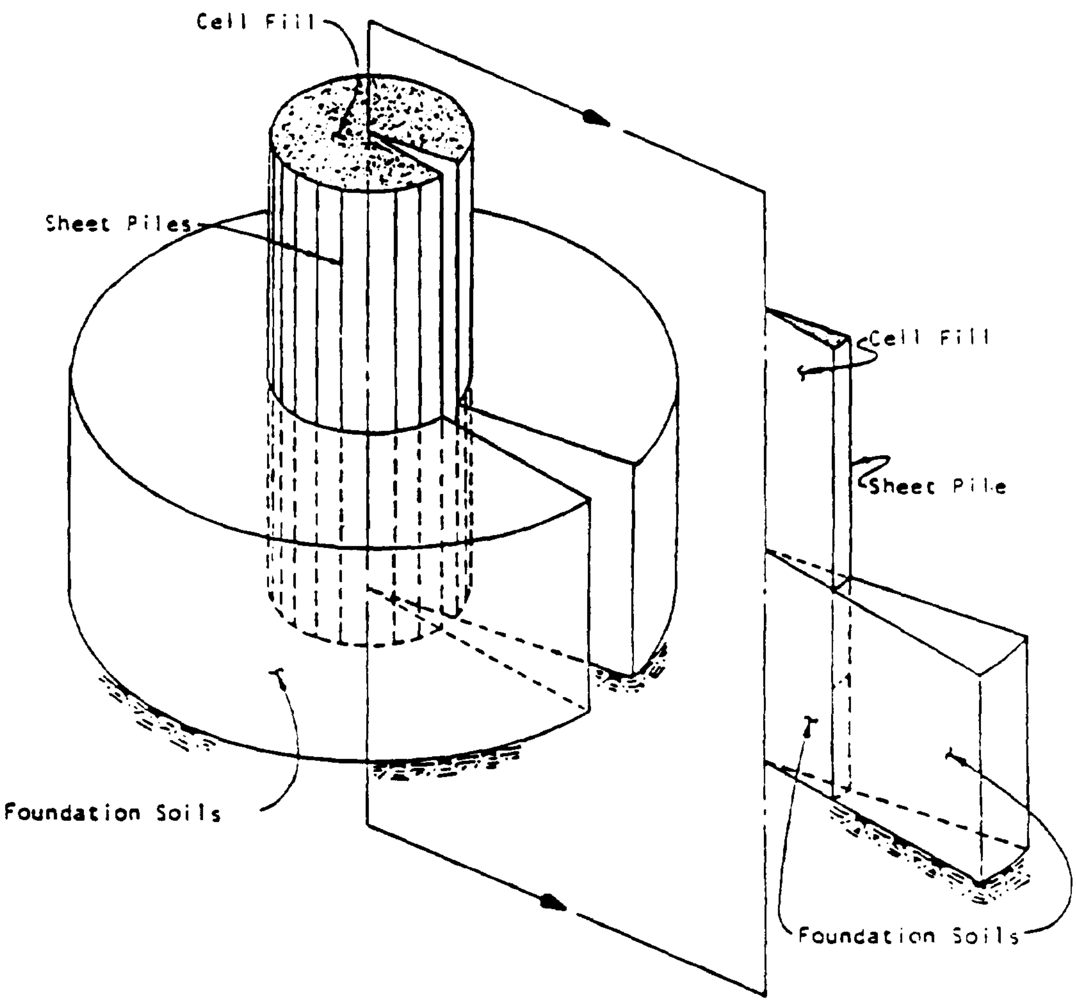

Figure 4-22. Schematic drawing, axisymmetric model

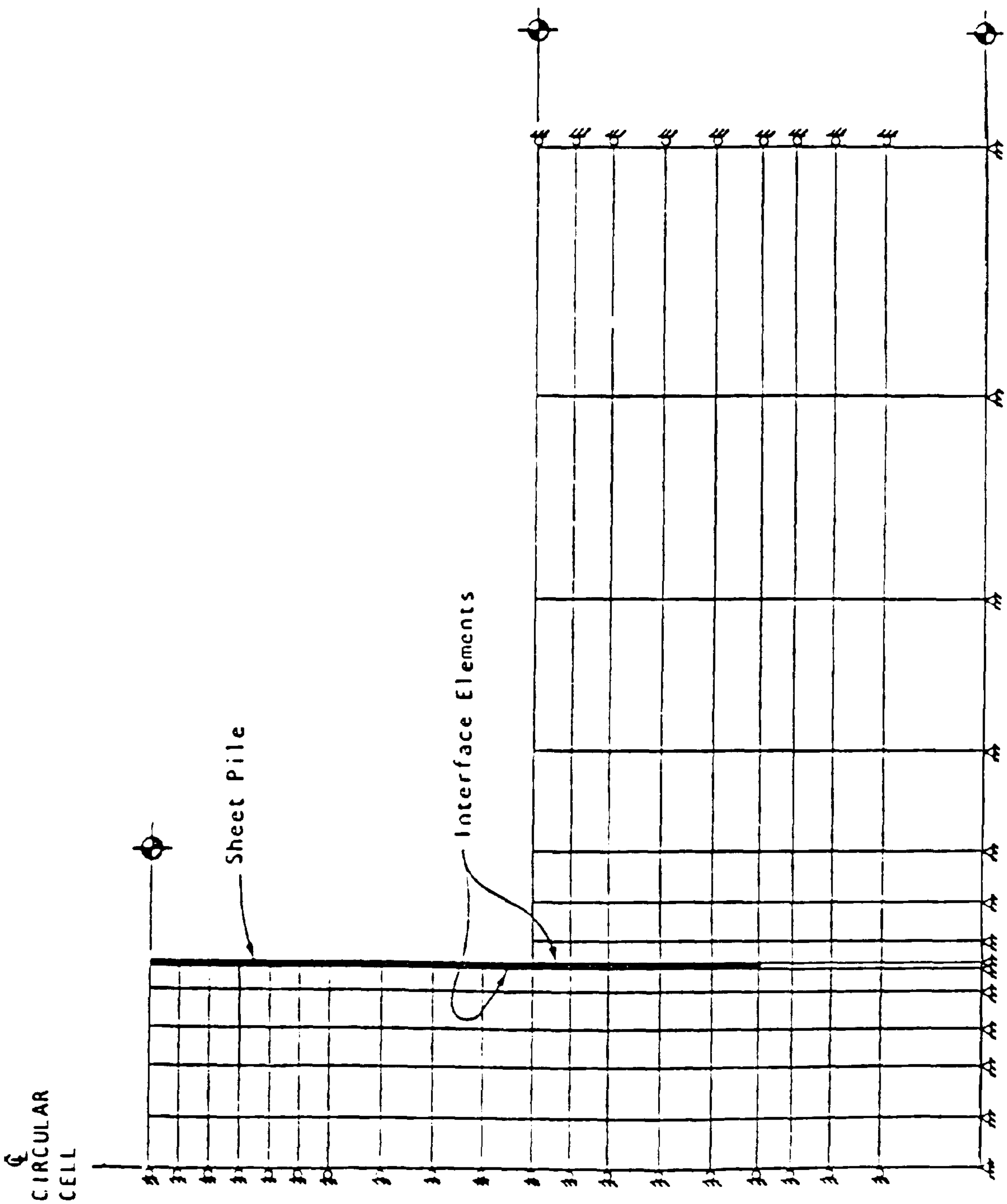

Figure 4-23. Finite element mesh for axisymmetric analyses of main cell filling

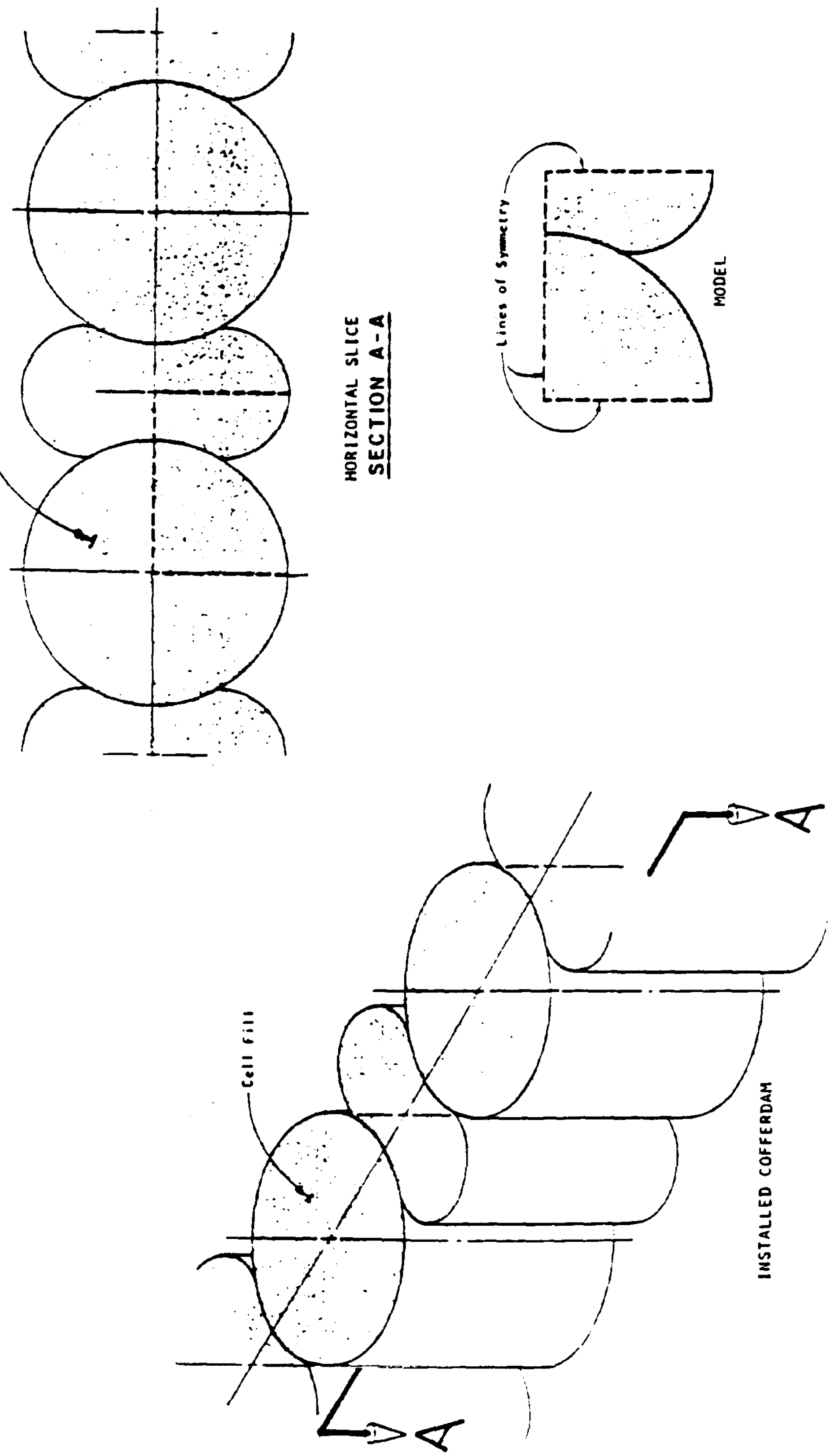

Figure 4-24. Schematic drawing, horizontal slice model

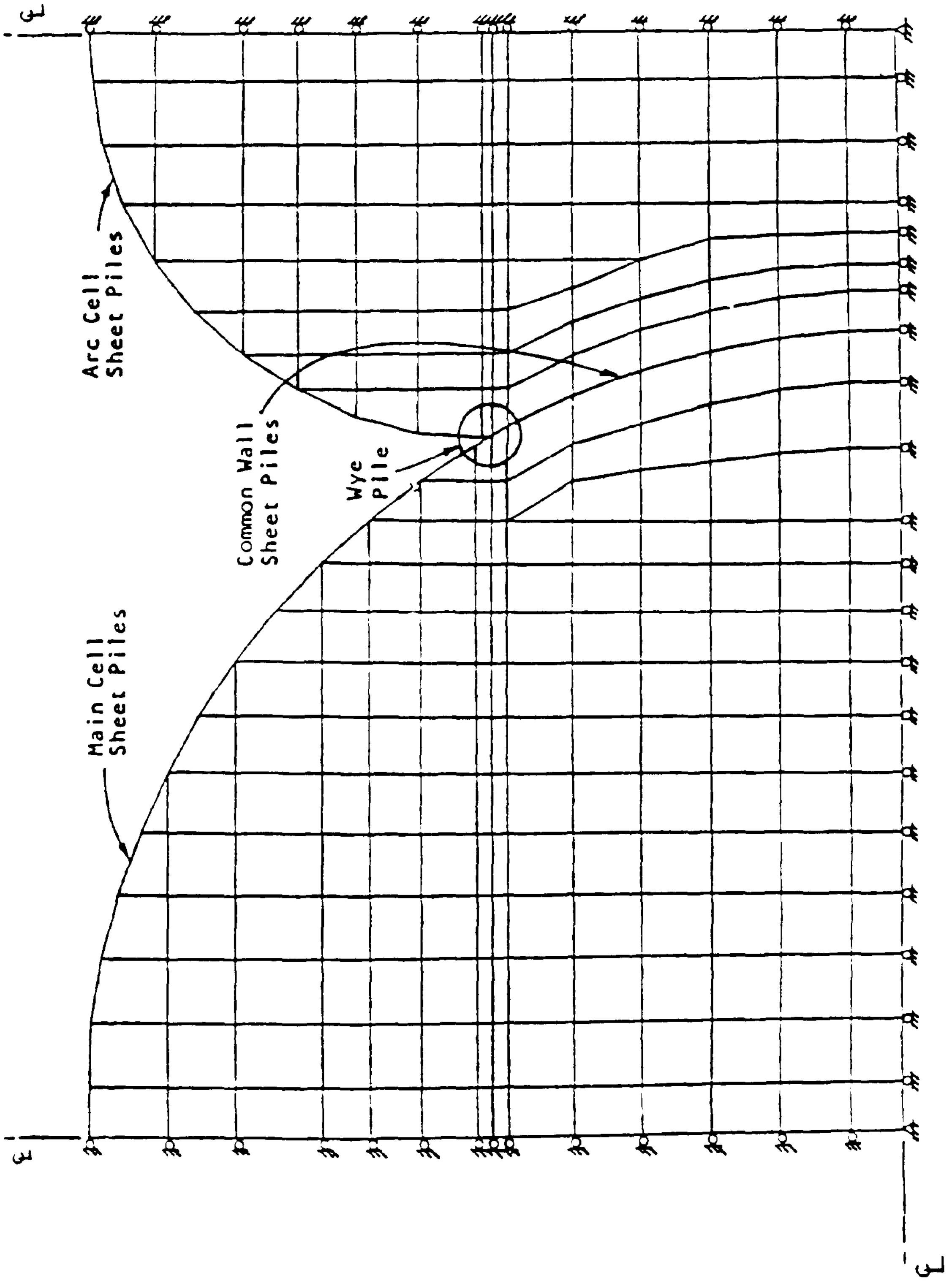

Figure 4-25. Finite element mesh for horizontal slice analysis of cell filling

d. General Modeling Techniques. Best results have been achieved on the three models by assuming the cell acts as an orthotropic shell by reducing the stiffness of sheet piles in the radial and circular directions during cell filling and acts as an isotropic material for all future construction steps. This is accomplished by reducing the modulus of elasticity in these directions. It is important for the analysis technique to breakdown the analysis into a series of incremental construction steps to allow deflections, settlement, and stresses to uniformly increase in the cell and foundation. Simulation of the actual sequence of loading is important because the stress-strain response of soil is nonlinear and stress-path dependent. All three model types are used in the Shannon and Wilson report.

4-20. Estimates of Cell Deformations.

a. Cell Buldging During Filling. During filling, the cell walls deflect outward as the fill pressures increase. This deflection in the radial direction, resisted by the sheet pile structure and foundation, causes the cell to form an area of maximum deflection and maximum interlock tension in the lower one third of the height above dredge line. This process of radial deflection transforms the cellular structure from a loosely pinned set of sheets into a structure more closely resembling a rigid cylinder. Because the cell is not a rigid cylinder the finite element model assumes that the sheet piles act orthotropically with less stiffness in the radial and circumferential directions than in the vertical. Three factors, other than stress-strain deflections, in the sheet piles support this assumption and contribute to higher deformations. First, interlocks are not perfect pins and gaps form in connections, The slack produced by gaps is taken up when pressure is applied to the inside of the cell by filling. Second, the interlocks provide a very small bearing area to transmit radial and circumferential forces from sheet pile to sheet pile. This allows for a small amount of rotation and local yielding in the interlocks. Third, due to the slack in the interlock it is possible for misalignment to occur during driving and, consequently, the cells have an irregular shape. The cells will tend to realign to a more perfect cylindrical shape during filling. To account for these deformations, the assumption of the cell's acting as an orthotropic cylinder is made by reducing the modulus of elasticity, horizontally and not vertically. In the Shannon and Wilson studies (item 69) at Lock and Dam 26 (Replacement), three different ratios of horizontal-to-vertical modulus were used in FEM solutions. These ratios were 1.0, 0.1, and 0.03. The E-ratio of 0.03 yielded results very close to actual field instrumentation. Vertical slice and axisymmetric models should be used for analyzing deflections during cell filling,

b. Deflections Produced by Berm Placement. Deflections of the filled cell during berm placement are normally small. Analysis of deformations for this stage can only be done using the vertical slice model and should be analyzed using uniform stages of berm construction. Previous FEM solutions in Lock and Dam 26(R) have shown slight deflections toward the outboard side of the cell of approximately 1 inch at the top. Soil stresses also increase on both sides of the sheet pile at the berm location and in the foundation soils under berm. Foundation pressure increases on the outside of the outboard side of the cofferdam indicate the filled cell is now acting as a unit and transferring inboard pressures through the circular cell to the outboard foundation.

c. Cofferdam Unwatering and Exterior Flood. Deflections and soil pressures resulting from cofferdam unwatering and exterior flood conditions are similar and, thus, are discussed together. Modeling of both conditions should be done by using a vertical slice model analysis and incremental load steps as the water level changes to allow for nonlinear soil deformations to take effect. Loads caused by seepage under the cofferdam should also be included using a flow net or uplift type analysis. From FEM modeling it can be seen that the cofferdam deforms by rotating and causing sliding forces toward the inboard side. These deformations increase the soil pressures in the cell fill and foundation directly under cell. Noted are higher soil pressures in the exterior foundation of the inboard side and in the berm due to passive soil resistance. Deflections of top of cell and high soil pressures in berm during exterior flooding indicate from previous analysis that the cell is moving as a unit with a tendency toward rotation for high exterior water levels. These model techniques are used in Lock and Dam 26(R) and Willow Island Cofferdam where, in addition to flood conditions, it was necessary to analyze an extra filling and unwatering of the cofferdam.

d. Construction Excavation. From previous analysis models, construction excavation has not been shown to cause significant cofferdam deformations except in the case of a cofferdam over a potential slip plane where excavation would reduce passive resistance to planar sliding. The potential slip plane should be modeled using frictional slip elements as shown by Clough and Hansen on the Willow Island Cofferdam study (item 18).

4-21. Structural Continuity Between Cells and Arcs. Cell and arc interaction can be analyzed by using a horizontal slice model and plane strain fill elements due to the perpendicular fill loading. A separate model analysis must be made at each elevation for which results are needed to obtain loads. Bar elements are used to represent sheet pile walls, with orthotropic material properties discussed earlier as bar properties. The Y-sheet pile connection between cell and arc should be modeled using exact piling widths as lengths of bar elements with pins at ends and at the Y-connection to more correctly simulate forces in the Y-connection. The simulation of construction steps for the horizontal model is loaded using results of the axisymmetrical model. This is due to the two-dimensional model's inability to account for arching in the cell and support provided by foundation passive resistance. Also, because of the model's inability to account for cell arching, fill stresses for each construction step must be obtained from the axisymmetrical analysis. Results for interlock tension and horizontal deflection that show close correlation to field instrumentation have come from this type of analysis. The horizontal model can only be used to analyze the symmetrical condition of cell filling. Only one study (item 69) of this type of analysis has been made to date, the Shannon and Wilson, Inc., Lock and Dam 26 (Replacement).

4-22. Structure--Foundation Interaction.

a. Foundation Stress at Cofferdam Base. Interaction between structure and foundation is modeled using a vertical slice analysis with a model cut wide enough and deep enough for foundation stresses to distribute evenly into foundation. The model should also include any planes of weakness in the foundation near the cofferdam. FEM analysis to date has shown foundation stresses are caused by two types of cofferdam action. First, due to filling of the cell, the sheet piles deflect outward and cause a buildup of passive resistance pressure in the foundation outside of the sheet piling. Vertical pressures in the foundation under the cell fill increase as a result of fill height above foundation. Second, after filling of the cell is completed, the cofferdam acts against horizontal forces as a monolithic cylinder resisting sliding by shear and passive pressures in the soil and overturning by the masses' resistance to tipping moment. The cell gains additional resistance to both sliding and overturning by the sheet pile's depth and, thus, interaction with the foundation.

b. Investigation of Foundation Problems. Investigation of foundation problems is one important advantage of FEM analysis. In cofferdam modeling, an element known as a planar frictional slip element can be used between elements to model a natural slippage plane between materials. These elements allow a buildup of shear stresses on the plane, and at an ultimate stress the two sides of the slip plane are allowed to slide in relation to each other. This action allows the adjacent element nodes to separate at the plane under a constant frictional resistance. These elements also have properties that will allow the two sides of the slip plane to pull apart, transverse to the plane, when placed in tension. Possible causes of foundation problems such as cofferdam dewatering, exterior flood, and interior excavation are failure load cases which should be investigated. A detailed description of use of this slip element is given in the Clough and Hansen study at Willow Island Cofferdam.

4-23. Fill Interaction Between Cells and Arc. Interaction of the main cell fill and arc cell fill has not currently been modeled due to cylindrical structure assumptions used in the vertical slice and axismmetric models. In the horizontal slice model the fill was assumed to be placed simultaneously in the main cell and arc which does not model the true sequence of construction. More research is needed in this area and would be more applicable for modeling with a three-dimensional soil-structure FEM analysis.

4-24. Special Cofferdam Configurations.

a. Cloverleaf Cells. Cloverleaf cofferdam cells at Willow Island were modeled in the Clough and Hansen study. The results of this analysis showed inconsistent patterns of deflection and indicated more research is needed. Part of the problem with modeling cloverleaf cells in two dimensions is accurately accessing the stiffness provided to the cell by center cross-walls.

b. Diaphram Cells. Past literature shows no attempts to analyze diaphram cells or other cell configurations by the FEM analysis. Development of a three-dimensional soil-structure finite element program with all of the necessary capabilities will enable modelers to more accurately analyze forces present in any special configuration of cell.

4-25. Research and Modeling Developments. Currently, research is being conducted by US Army Engineer Waterways Experiment Station (WES), Information Technology Laboratory (ITL), formerly Automation Technology Center (ATC), to develop a Corps of Engineers three-dimensional, soil-structure finite element program. With all of the capabilities necessary to model cellular cofferdams, the program will be tested on the Lock and Dam 26 (Replacement) cofferdam, since it is the most extensively instrumented cofferdam of current practice.